NATAL KICKS OF NEUTRON STARS

Andrei Igoshev
University of Leeds

In collaboration with:
Frank Verbunt, Eric Cator,
Martyna Chruslinska, Andris Dorozsmai
and Silvia Toonen

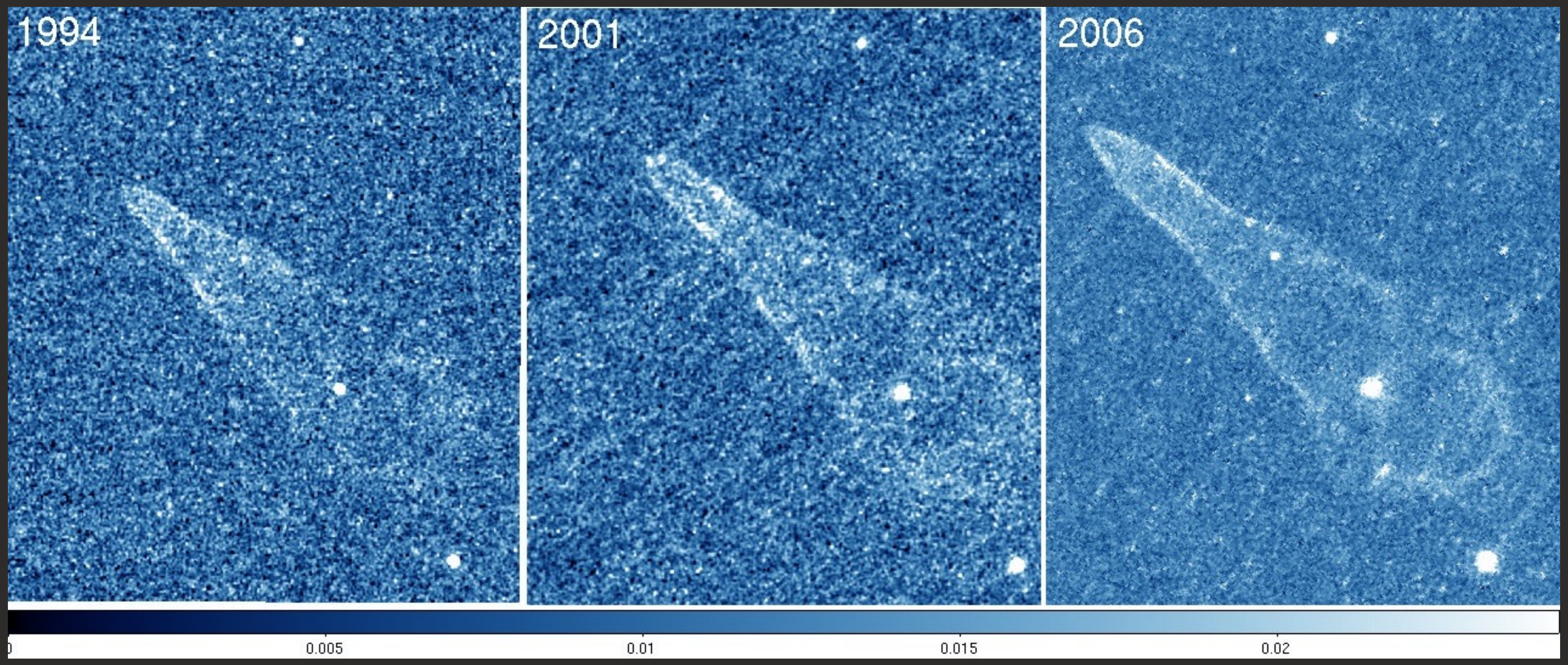

OUTLINE

- Distances of NSs
- Velocities of isolated radio pulsars
- Velocities of NSs born in binaries

DISTANCES ARE ESSENTIAL TO UNDERSTAND NS PHYSICS AND MILKY WAY

- Estimate of NS velocity
- Estimate of NS X-ray, gamma or radio luminosity
- Density of interstellar medium
- Magnetic field of interstellar medium

VELOCITIES ARE ESSENTIAL TO LEARN ABOUT THE SUPERNOVA AND NS PHYSICS

- Estimate of age
- Estimate of fraction of NS in globular clusters
- Double NS merger rate
- Physics of supernova explosion: electron capture, symmetric

HOW DO WE MEASURE DISTANCES?

- Parallax - VLBI only: typical distances < 1 kpc
- Pulsar timing
- Dispersion measure and a model of the electron density in the Galaxy
- Upper limit from absorption lines of neutral hydrogen
- X-ray flares
- Spectral fitting of binary companion

HOW DO WE MEASURE DISTANCES?

- Parallax - VLBI only: typical distances < 1 kpc
- Pulsar timing
- Dispersion measure and a model of the electron density in the Galaxy
- Upper limit from absorption lines of neutral hydrogen
- ~~X-ray flares~~ Works only for some neutron stars
- ~~Spectral fitting of binary companion~~

PULSAR TIMING

Good solution

Error in position

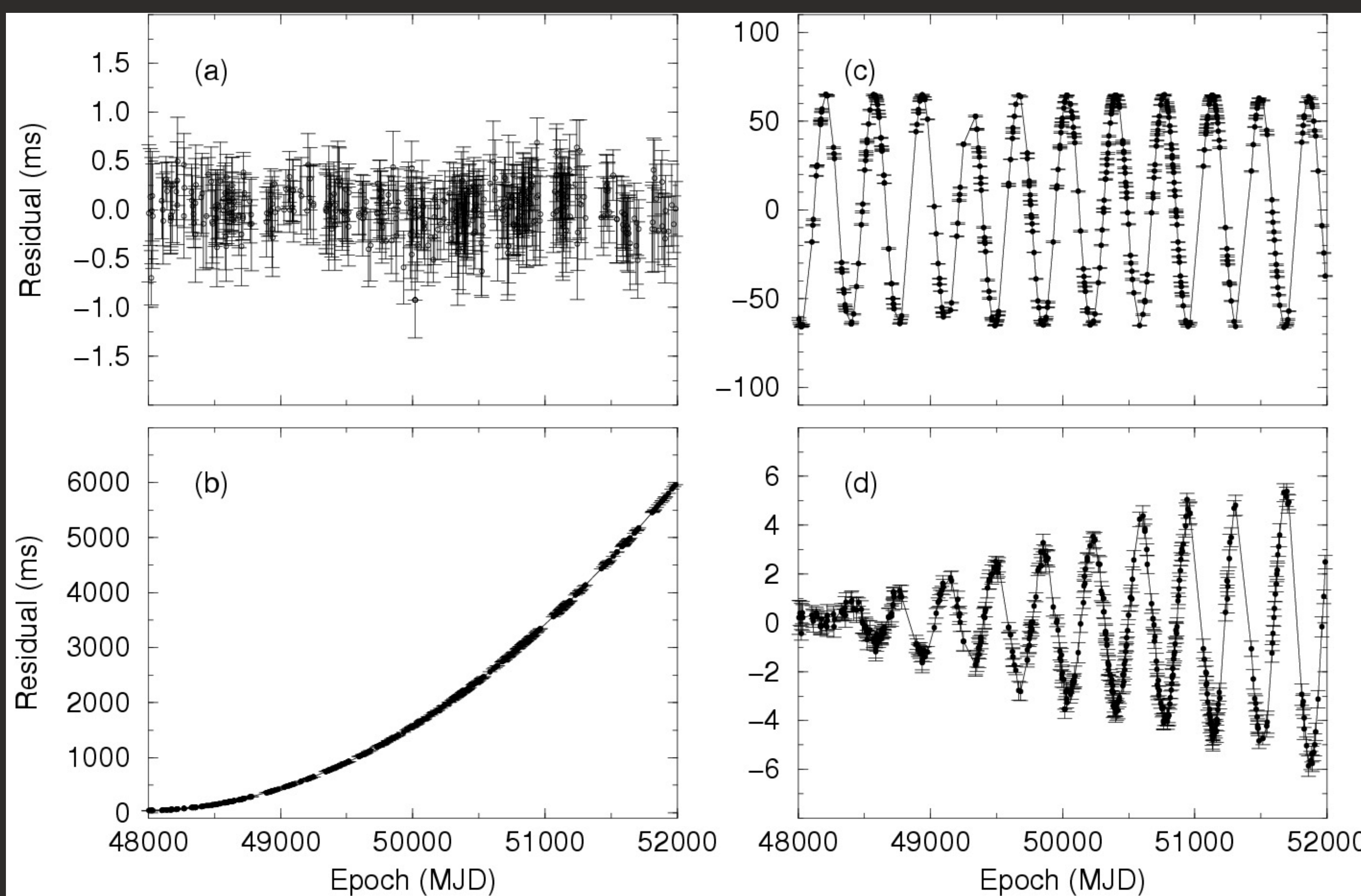

Error in frequency derivative

Error in proper motion

- In this technique, the time of arrival of individual pulses on long timespan (~10 years) is studied.
- To predict the time of arrival we need to know the solar system ephemeris, source stellar coordinates, its magnetic field and its motion.

Lorimer & Kramer (2005)

DISPERSION MEASURE (DM) USING THE ELECTRON DENSITY MODEL

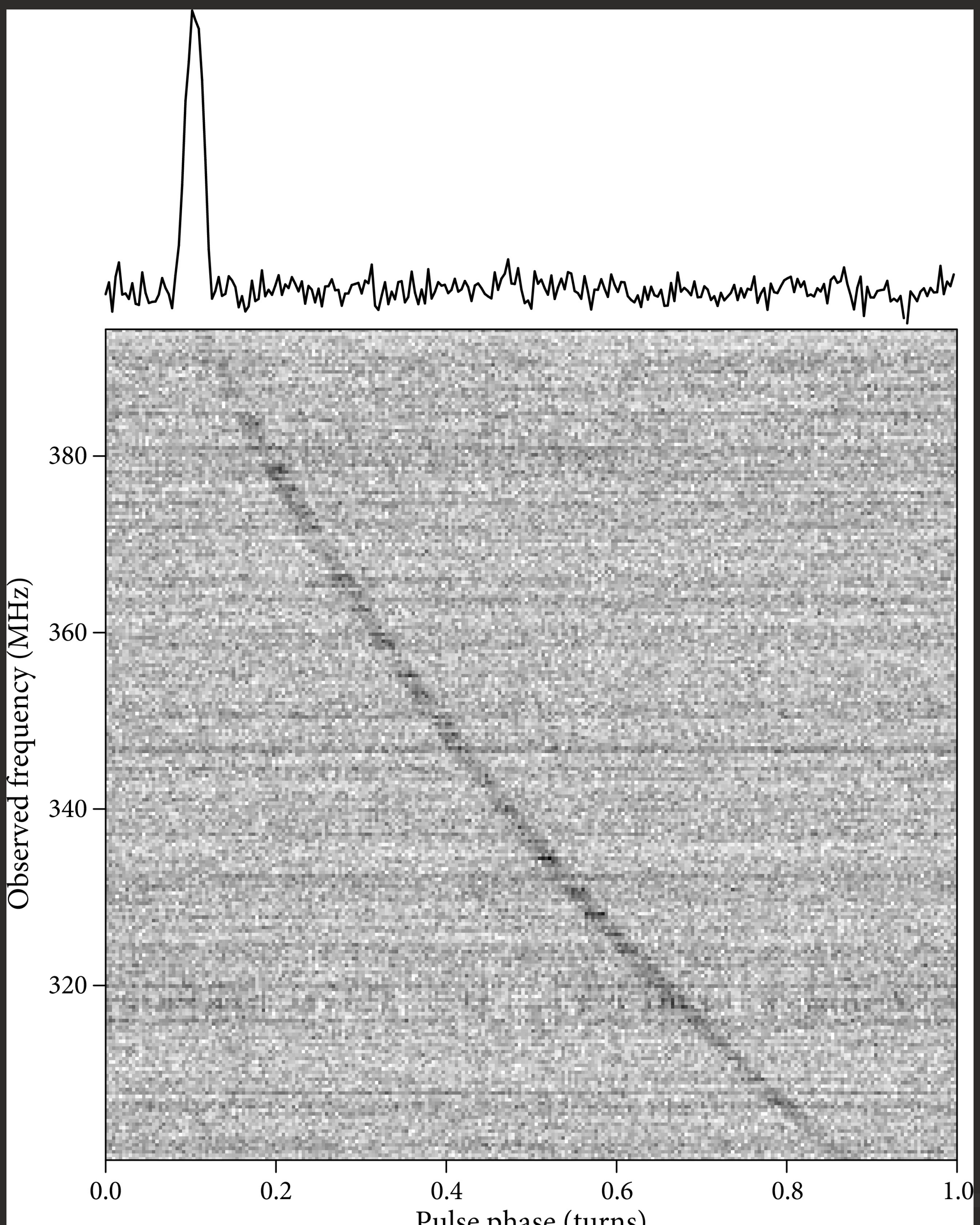

Dispersion measure is the delay between arrival of the radio pulse at different frequencies caused by the dependence of the refractive index of cold interstellar plasma

Cordon & Ramson (2015) Essential radio astronomy

MODEL OF ELECTRON DENSITY FOR MILKY WAY

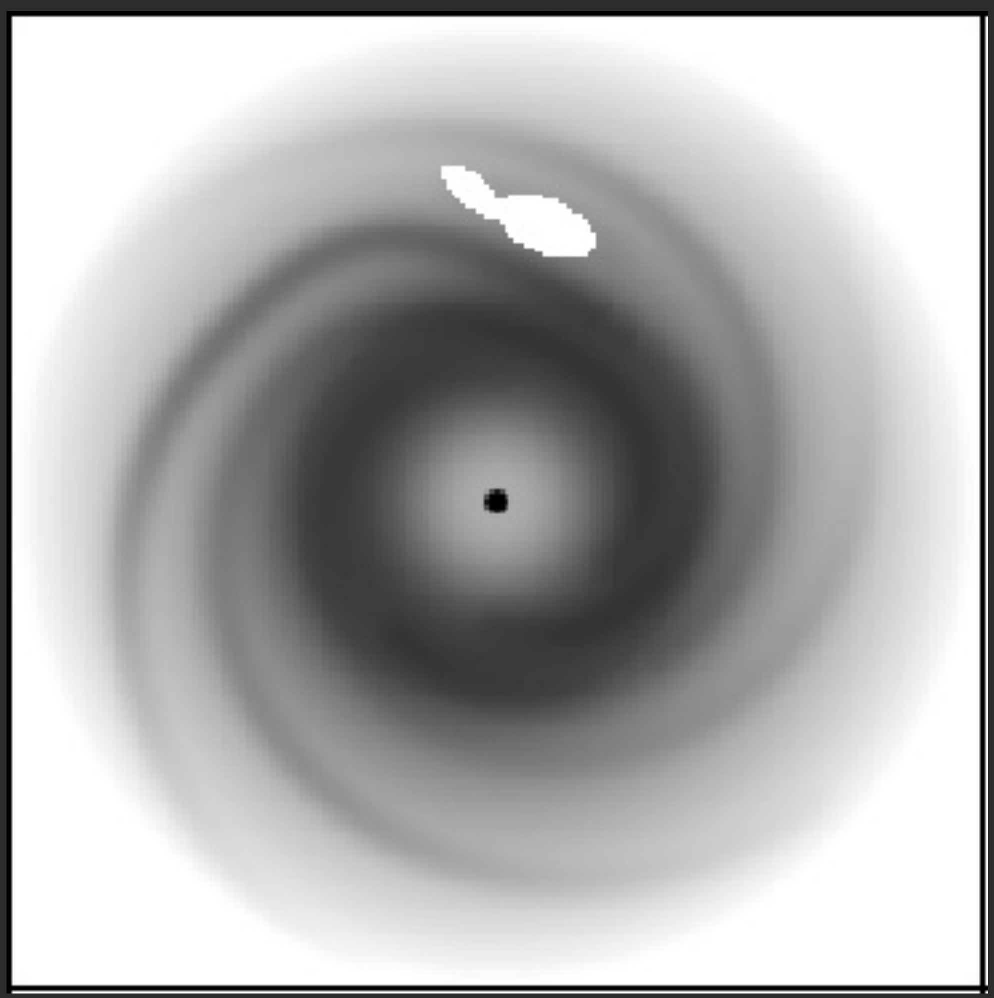

Free electron density

NE2001: Cordes & Lazio (2001) arXiv:0207156

- Constant development, the first suggestions immediately after the first pulsar discovery: Hewish et al. (1968)
- The most cited: Taylor & Cordes (1993) - the main advantage is simplicity. No parallax data were used to construct it.
- Combination of local effects (the Gum nebula) and global matter distribution in the Galaxy.
- NE2001 includes a lot of structure.

NEW MODELS OF ELECTRON DENSITY FOR MILKY WAY

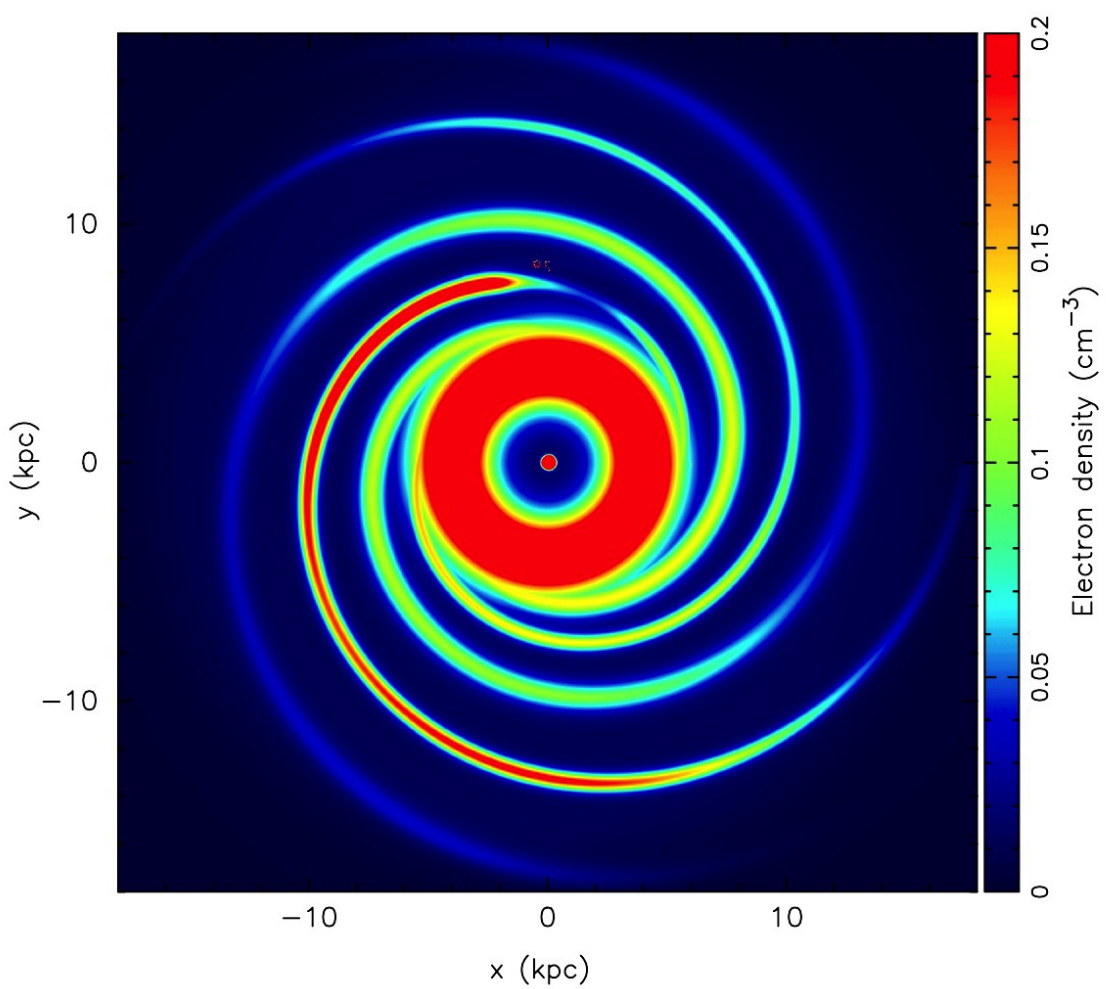

Yao, Manchester and Wang (2017)

- Recent development: Schnitzeler (2012) - a fit of Taylor & Cordes (1993) model to modern data.
- Yao, Manchester & Wang (2017) - YMW model. The model is written in C++.
- http://119.78.162.254/dmodel/index.php

QUALITY OF ELECTRON DENSITY MODELS

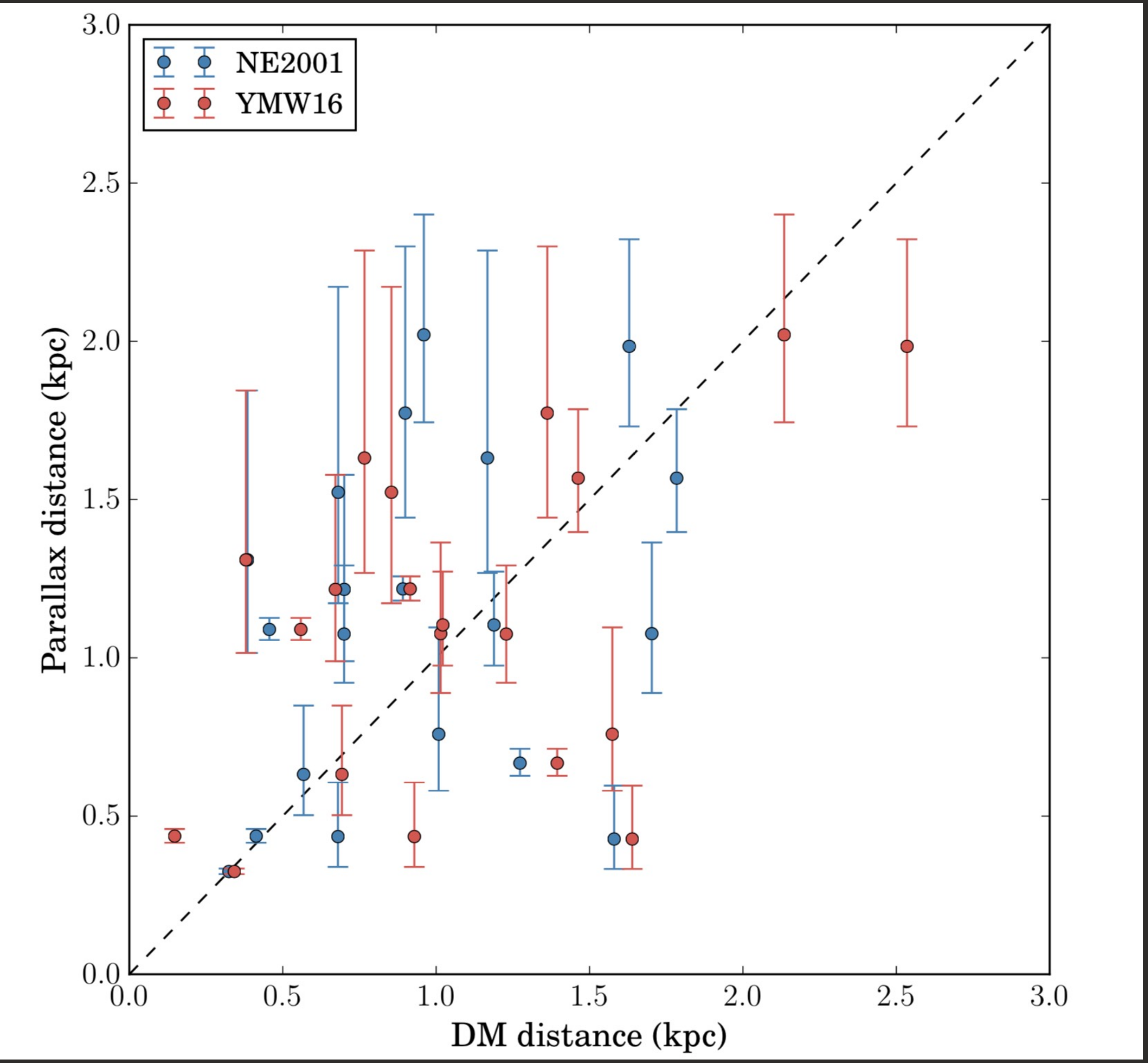

- It is challenging to introduce a reliable error distribution. Starting from TC93 people cite 20% error bars on distance derived from models.
- Comparison of new parallax measurements with the distances estimated from DM gives up to 2.5 times difference.

Arzoumanian et al. (2018)

QUALITY OF ELECTRON DENSITY MODELS

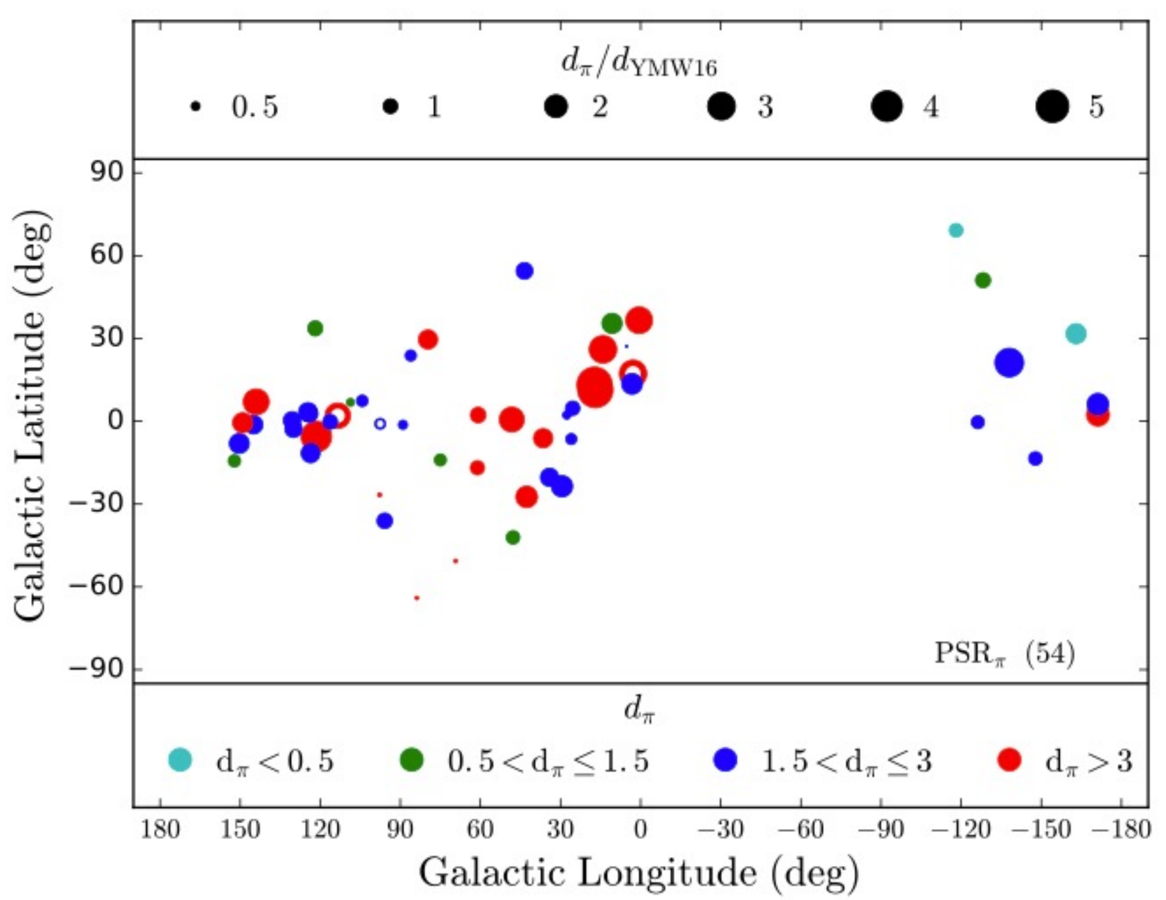

Figure 14. Ratio of VLBI parallax distance to the NE2001 model distance (top panel) and the YMW16 model distance (bottom panel). The results are shown as a function of Galactic longitude and latitude. Circle sizes indicate the value of the ratio, as shown in the upper legend in each panel. Circle colors denote parallax distance in kpc as in the lower legend in each panel. Filled circles denote distance measurements, while the three open circles indicate lower bounds on pulsar distances.

Deller et al. (2019)

- Difference could be 5 times between the distance estimated by parallax and by using YMW16 model.

LET SUGGEST THAT WE KNOW PARALLAX, WHAT ARE ERRORS?

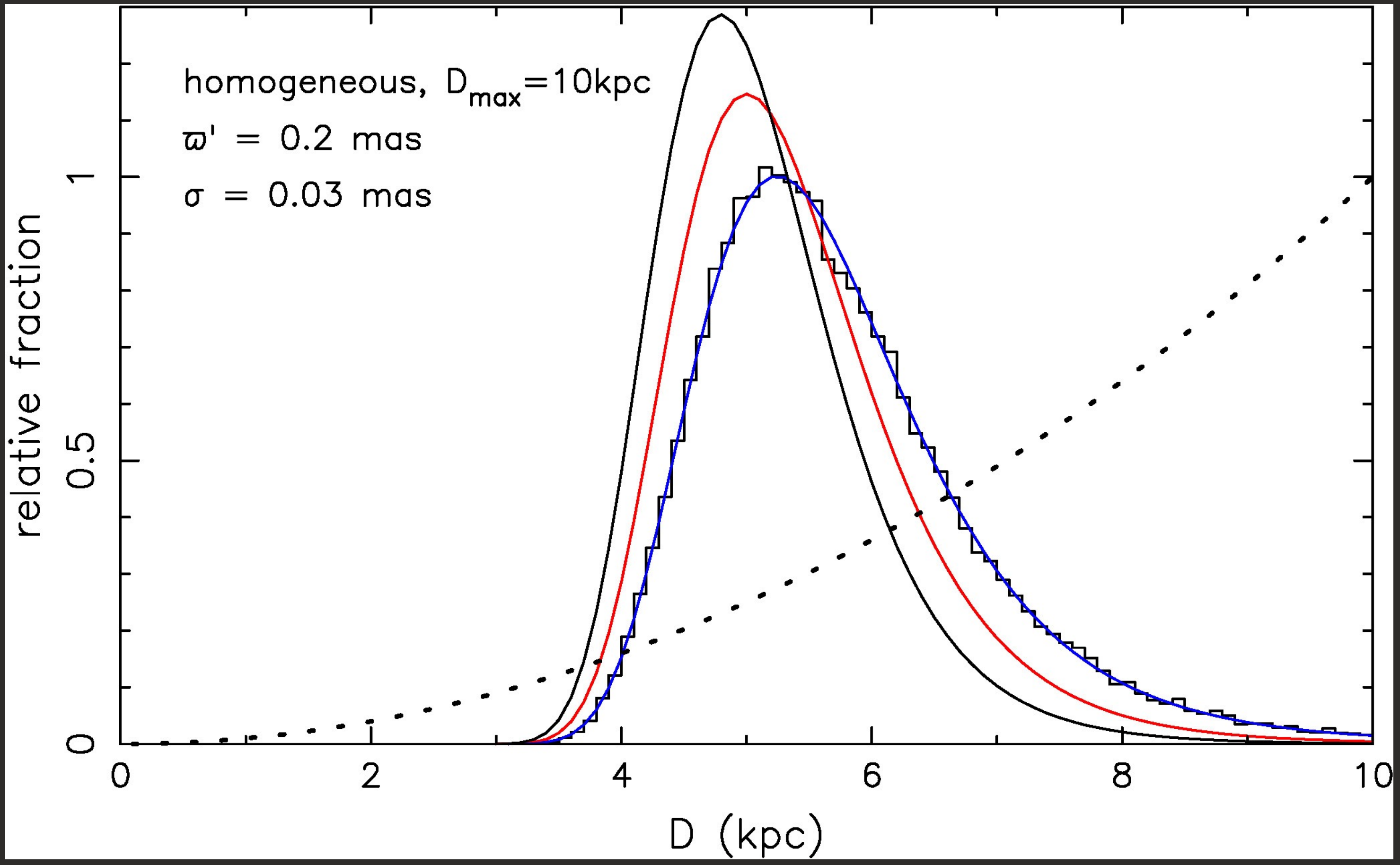

- Distance is not measured when the parallax is measured.
- The error in parallax appears because of the instrument limitations.
- Errors of distance are combinations of the instrumental limitations and internal distribution of objects.
- Need Bayesian technique

Igoshev, Verbunt & Cator (2016)

HOW TO ESTIMATE THE DISTANCE UNCERTAINTY PROPERLY?

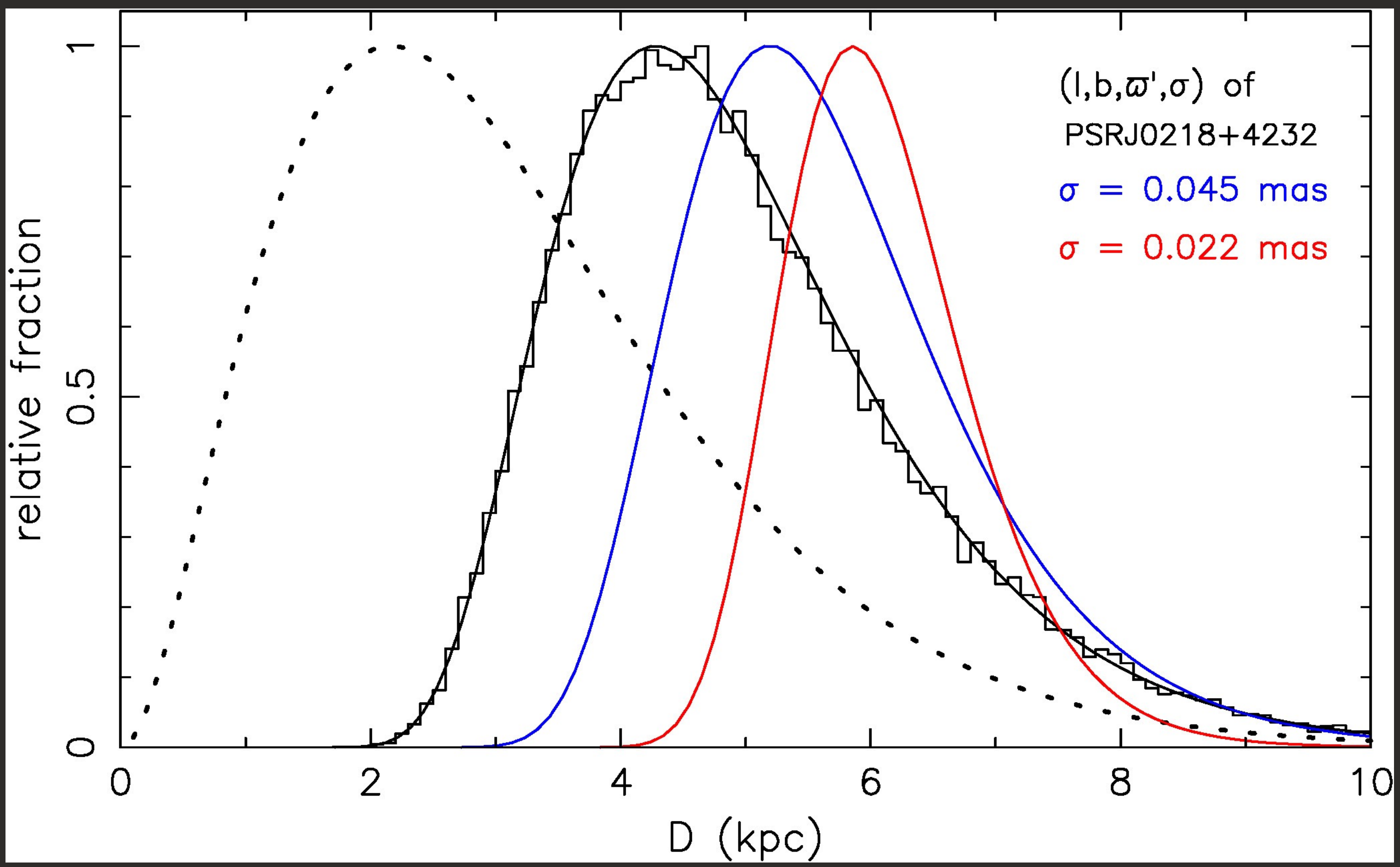

Igoshev, Verbunt & Cator (2016)

- Estimate of the probability distribution for derived quantity always requires prior.
- Use bound prior with exponential cut-off: Bailer-Jones (2017) "Practical Bayesian inference".
- In a case of pulsars, we can use the distribution of pulsars in the Galaxy. It depends on direction.

HOW DO WE MEASURE NS VELOCITY?

- We can measure velocity (radial) only for a NS in a binary observing the secondary star and fitting its spectrum.
- All other techniques provide proper motion.
- Proper motion is two out of three velocity components.
- To get velocity, the proper motion must be combined with distance.

SOME NEUTRON STARS ARE VERY FAST

- The guitar nebular.

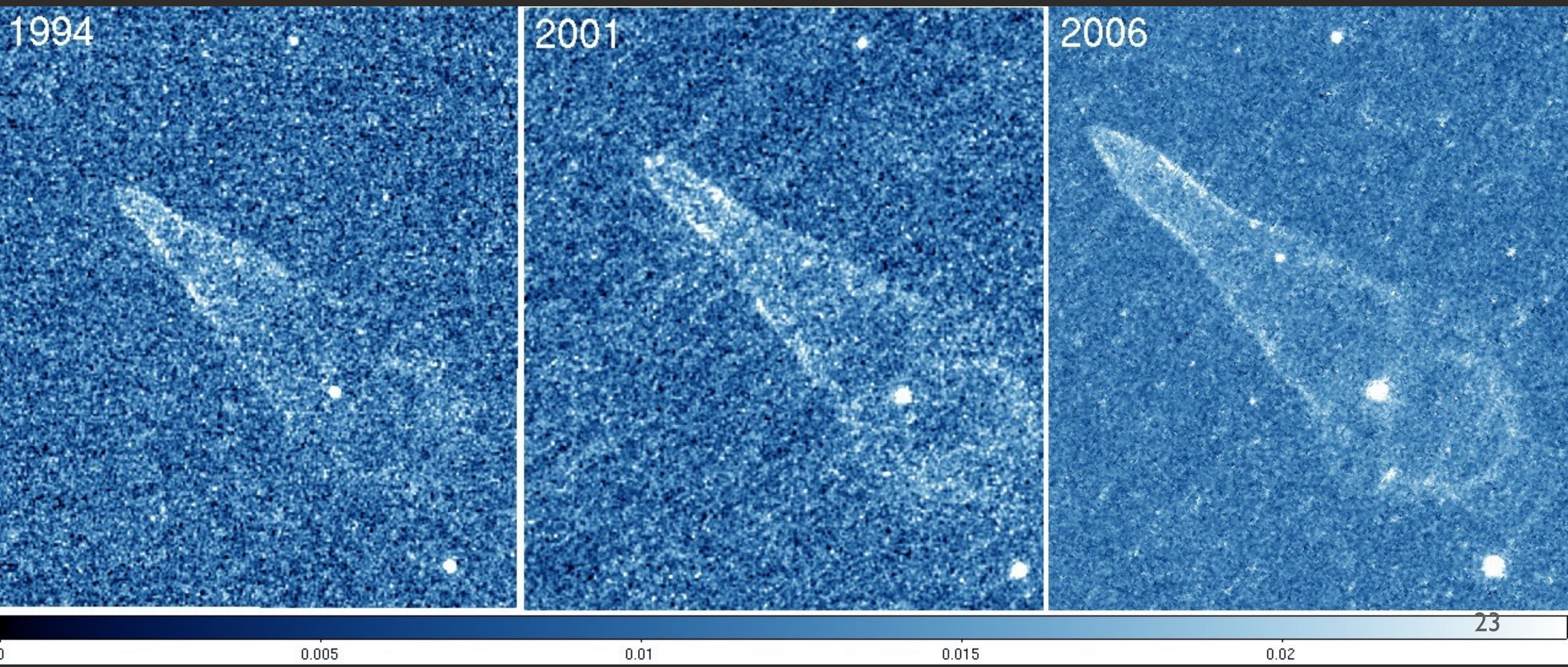

Chatterje et al. 2006

SOME RADIO PULSARS ARE EXTREMELY SLOW

Radio pulsars in Terzan 5.

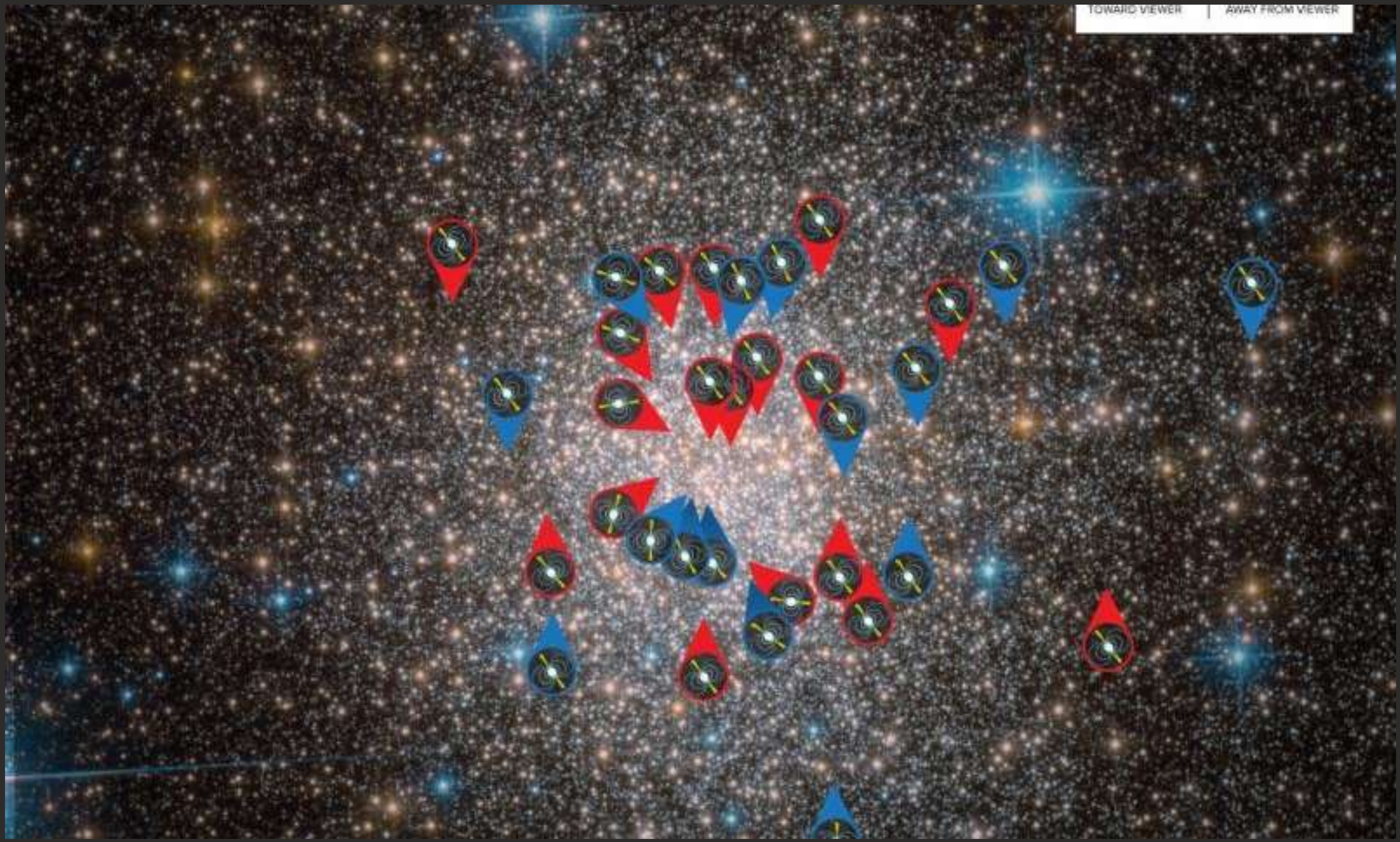

Prager et al. (2017)

THE KNOWN VELOCITY DISTRIBUTION LACKS BOTH

- Known velocity distribution fails to account for both high and low-velocity objects.

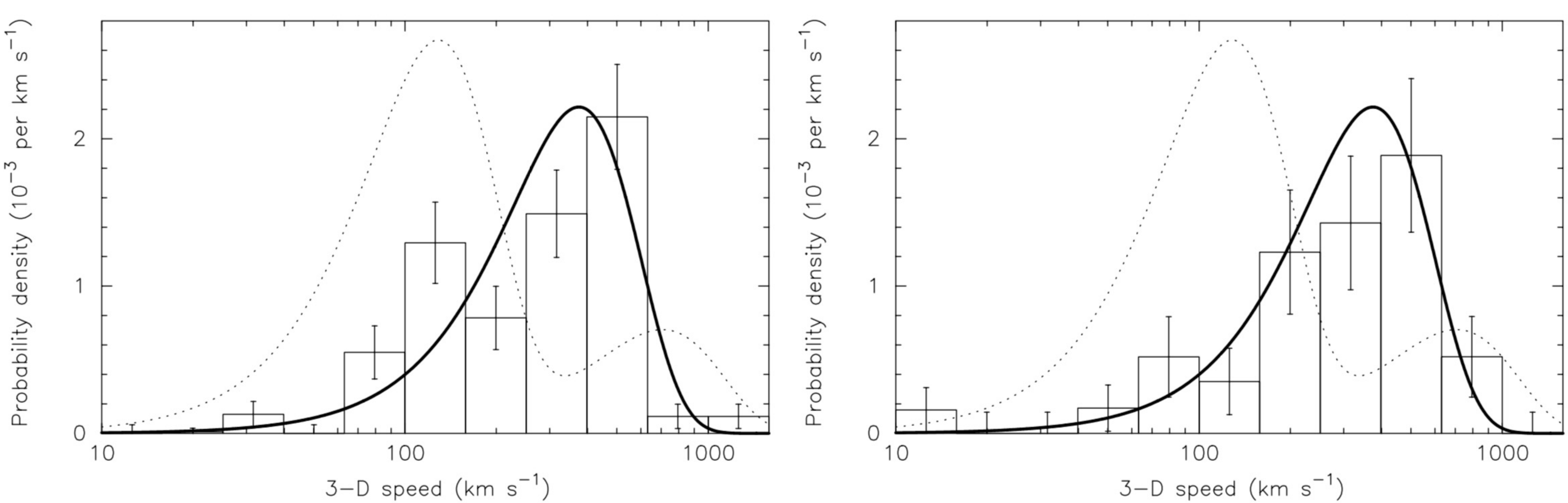

Hobbs et al. (2005)

OUR APPROACH TO PULSAR VELOCITIES

- We use only recent (after 2000) VLBI measurements of parallax and proper motion.
- We correct for the Local Standard of Rest (LSR) assuming that young pulsars (age < 10 Myr) didn't move far away from their birth location.
- We study the velocity distribution above the LSR.

EQUATION FOR LIKELIHOOD

Parallax

Proper motion in RA

Proper motion in DEC

$$P_{\mathrm{maxw}}(\varpi', \mu'_{\alpha*}, \mu'_{\delta}, D, v_{\alpha}, v_{\delta}, v_r) = G(v_{\alpha}, \sigma)G(v_{\delta}, \sigma)G(v_r, \sigma)$$

$$\times \quad \frac{f_D(D)}{\int_0^{D_{\max}} f_D(D)dD} \frac{1}{\sigma_{\varpi}\sqrt{2\pi}} \exp\left[-\frac{(1/D - \varpi')^2}{2\sigma_{\varpi}{}^2}\right]$$

$$\times \quad \frac{1}{\sigma_{\alpha}\sqrt{2\pi}} \exp\left[-\frac{(\mu_{\alpha*,G}(D) + v_{\alpha}/D - \mu'_{\alpha*})^2}{2\sigma_{\alpha}{}^2}\right]$$

$$\times \quad \frac{1}{\sigma_{\delta}\sqrt{2\pi}} \exp\left[-\frac{(\mu_{\delta,G}(D) + v_{\delta}/D - \mu'_{\delta})^2}{2\sigma_{\delta}{}^2}\right]$$

G - gaussian

$$L_{\mathrm{maxw}}(\sigma) = \int_o^{D_{\max}} \int_{-\infty}^{\infty} \int_{-\infty}^{\infty} \int_{-\infty}^{\infty} P_{\mathrm{maxw}} dv_{\alpha} dv_{\delta} dv_r dD$$

COMPLETE ANALYSIS: MAXIMUM LIKELIHOOD TECHNIQUE

$$\mathcal{L}(\vec{\sigma}) = -2\sum_{i=1}^{N} \ln L_i(\vec{\sigma})$$

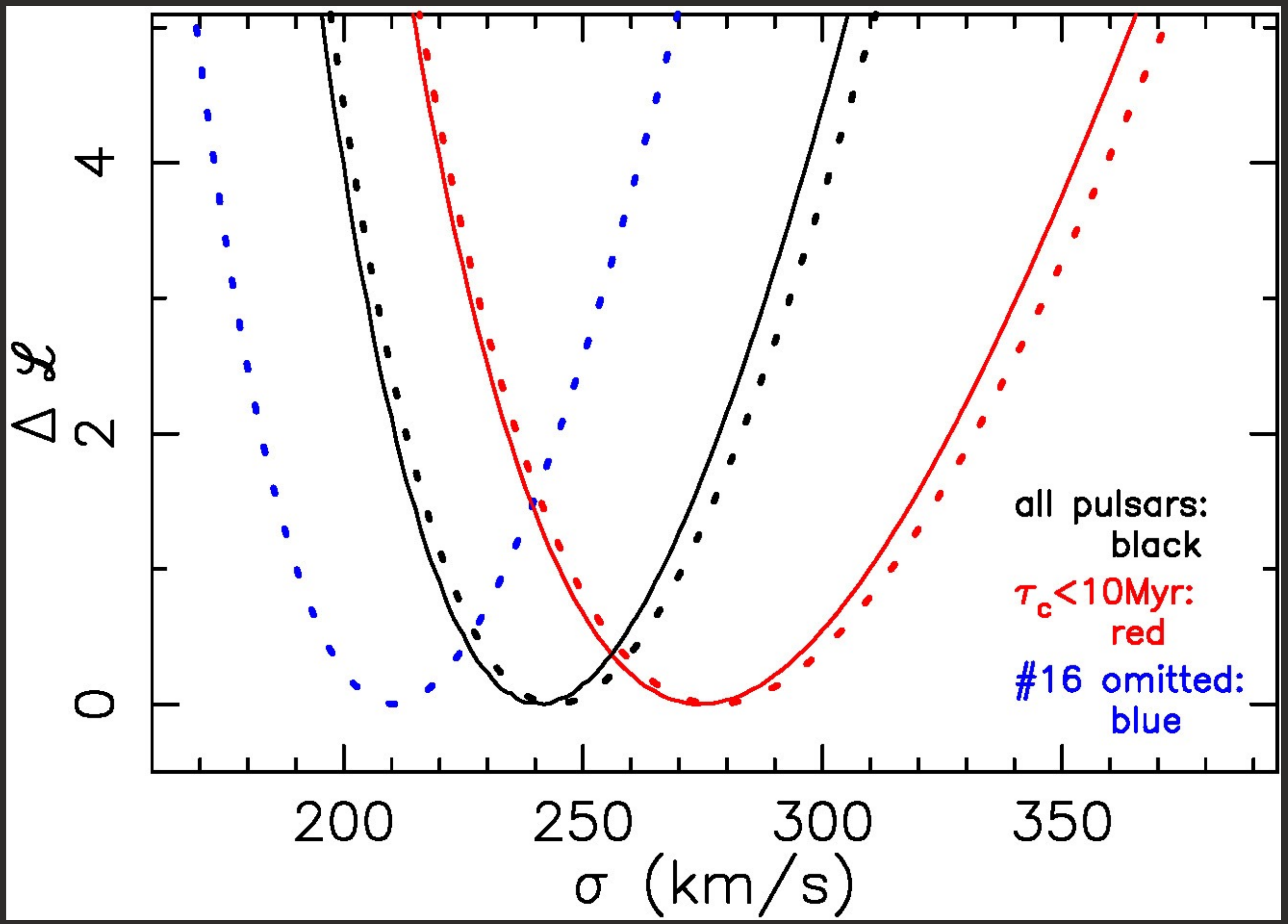

- We introduce a likelihood, which is a function of model parameters.
- The total likelihood is a product of likelihoods for individual pulsars (conditional probability of getting a measurement if the model is given).
- To find a parameter which describes sample the best we optimise the likelihood.

Verbunt, Igoshev & Cator (2017)

RESULTS OF ANALYSIS

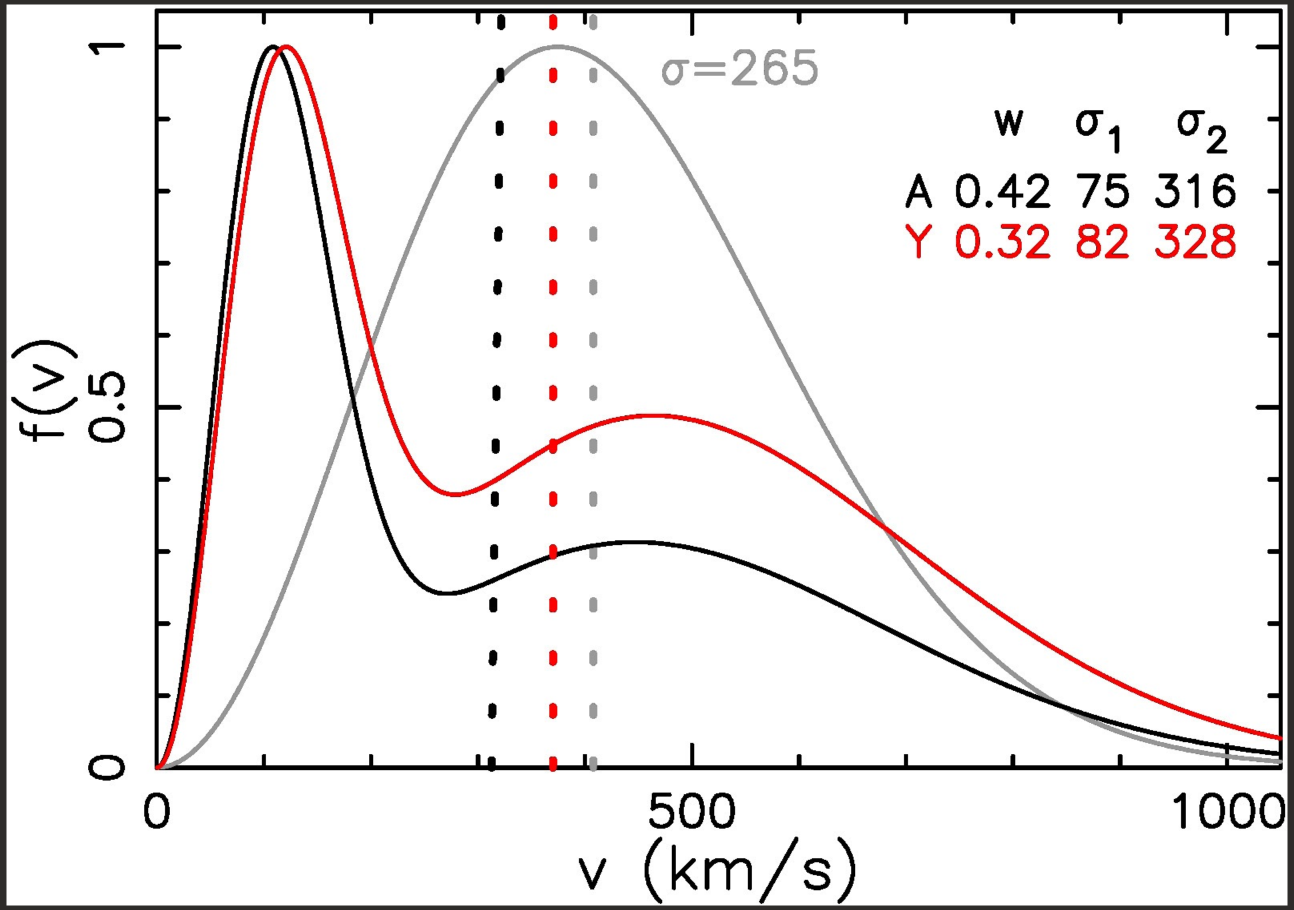

- It is bimodal, one peak at 75 km/s and the second peak is at 316 km/s.
- If we exclude any pulsar from consideration, it does not change.
- 3%-5% of pulsars have velocities at birth less than 60 km/s (retain in globular clusters).

Verbunt, Igoshev & Cator (2017)

WHY IS IT SO DIFFERENT FROM HOBBS ET AL. (2006)?

- Hobbs et al. (2006) used the distances estimated through the NE2001 electron density model (errors up to 3 times of the distance value). Significant errors in distance lead to overestimating of velocities.

- Hobbs et al. (2006) didn't take into account the observational uncertainties.

- Hobbs et al. sample is much larger (hundreds of objects), but the errors for proper motion are two orders of magnitude larger.

$$\sigma \propto \frac{1}{\sqrt{N}}$$

- The error is usually inversely proportional to square root of sample size. So, the consideration of small sample of the best measurements available still provides a better estimate for velocity distribution.

NEW CATALOGUE: COMPLETE PSRπ

- Deller et al. (2019) published a much larger sample of VLBI measurements for parallaxes and proper motions of radio pulsars.

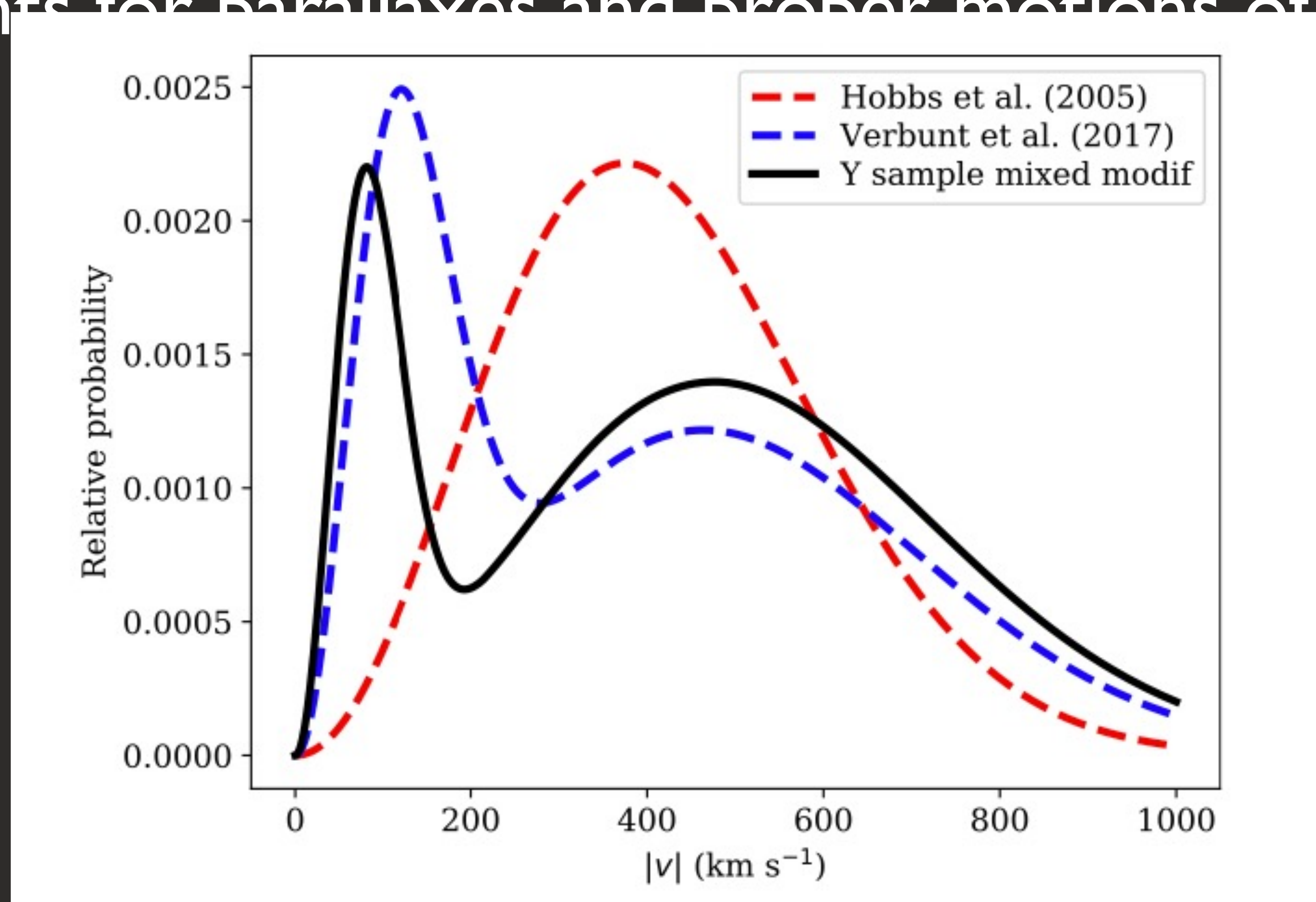

Igoshev (2020)

CONCLUSION

- To estimate the uncertainty for a derived quantity, the Bayesian framework must be used. Any explicit prior is better than an implicit one.
- In the case of low-quality parallax measurements, a realistic galactic prior must be used to estimate the physical properties related to the distance correctly.
- The velocity distribution of isolated radio pulsars is bimodal with σ = 56 km/s and σ = 336 km/s, and the first component contains 20% of objects. A fraction of neutron stars retained in globular clusters is in range 5±3%

Natal kick of NS based on simulations and observations of Be X-ray binaries

Be X-ray source

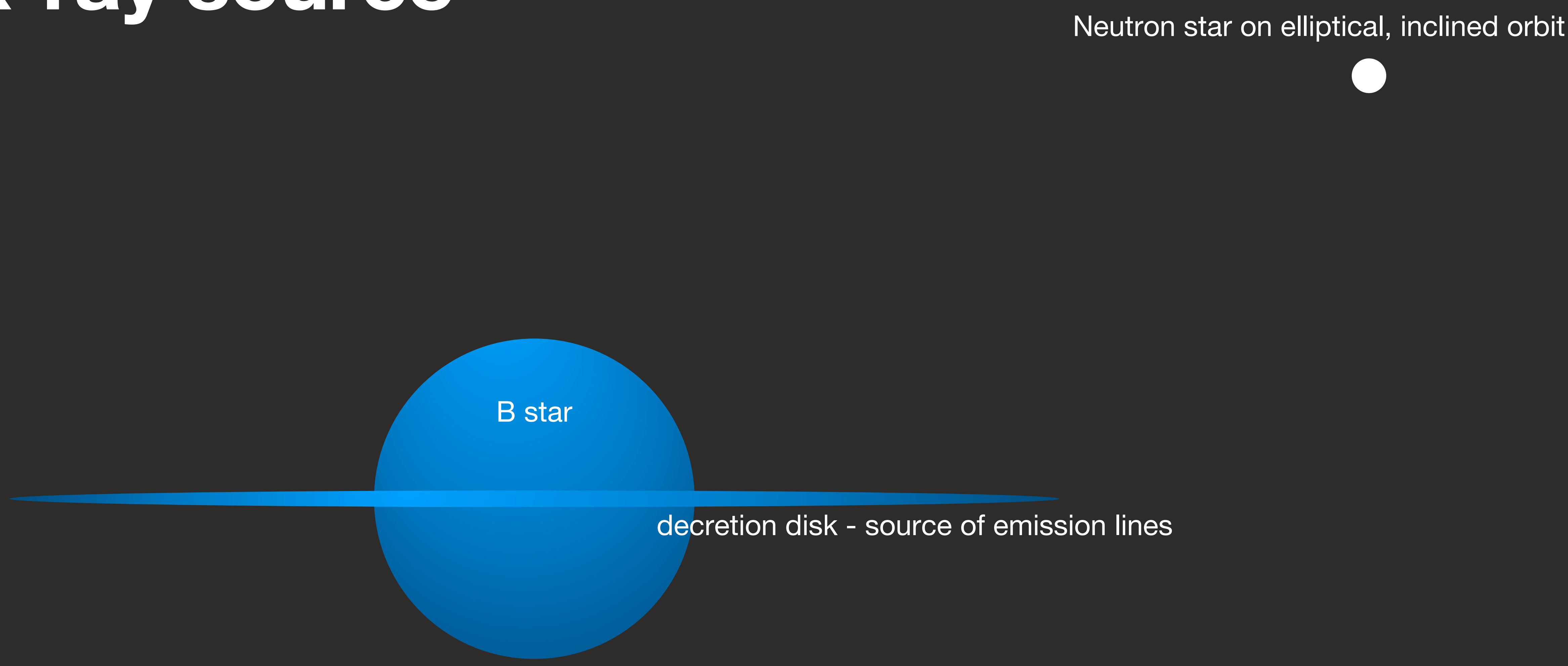

Be X-ray source

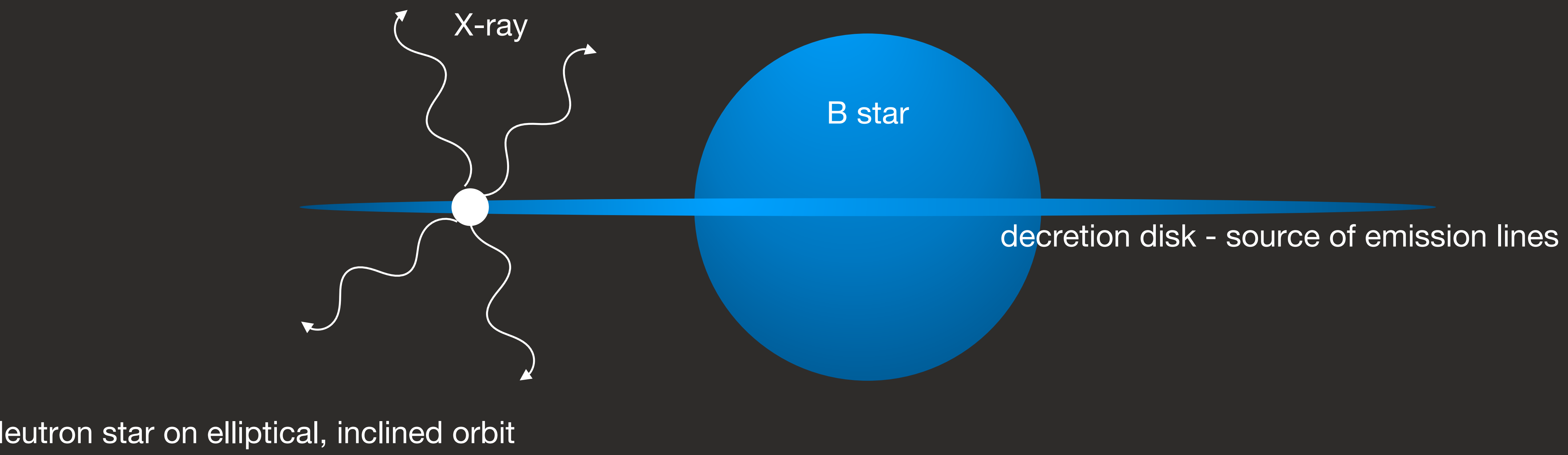

Be X-ray source

Essential selection effects:

- In too wide systems the NS does not enter the decretion disk: no X-ray emission
- Eccentricities are hard to measure
- In SMC, there is a strong observational bias against detecting wide systems (period longer than 500 s) and measuring their orbital periods
- In widest systems, the NS might avoid the decretion disk, so never seen in X-ray.

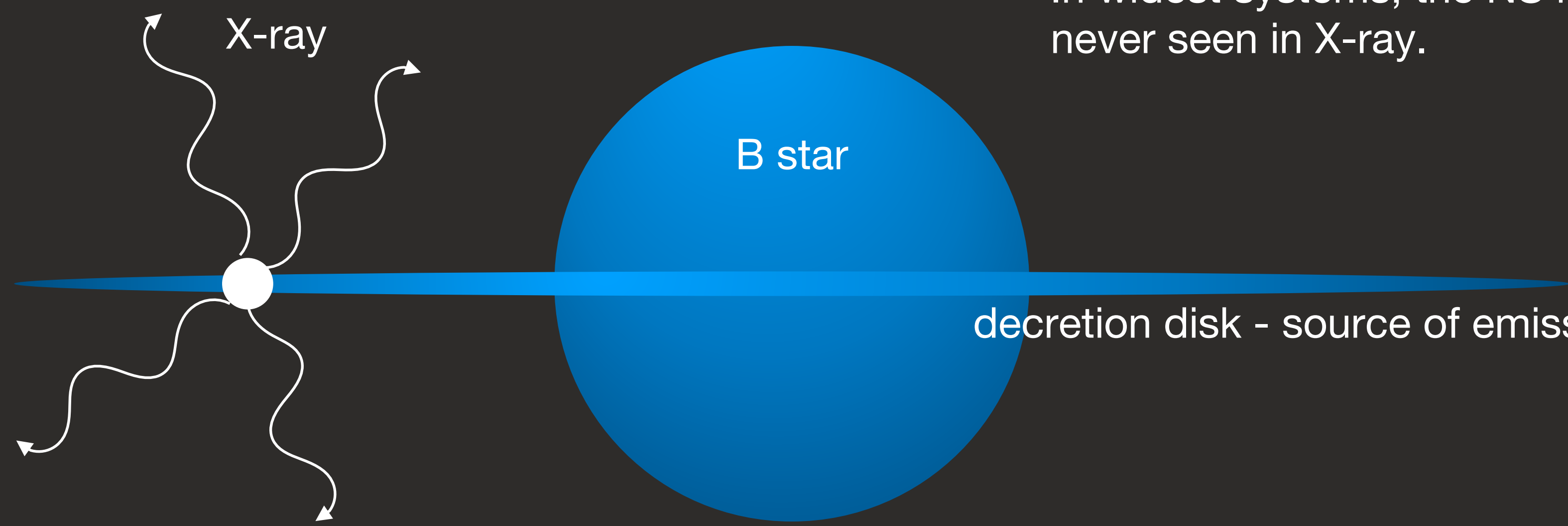

Motivation

All normal radio pulsars with measured parallaxes and proper motions are isolated.
Most of normal radio pulsars (>94%) are isolated as well (Antoniadis 2020a,b)
If assume that all NS are born initially in binaries, ones with weak natal kick are much more probable to stay bound than ones with e.g. Hobbs natal kick.

Natal kick distribution	System after NS explosion Bound	Unbound
No kick	0.74	0.26
Hobbs et al. (2005)	0.042	0.958
Igoshev (2020)	0.07	0.93

When we look at a binary with NS it is up to 10-20 times more probable that this NS received weak natal kick.

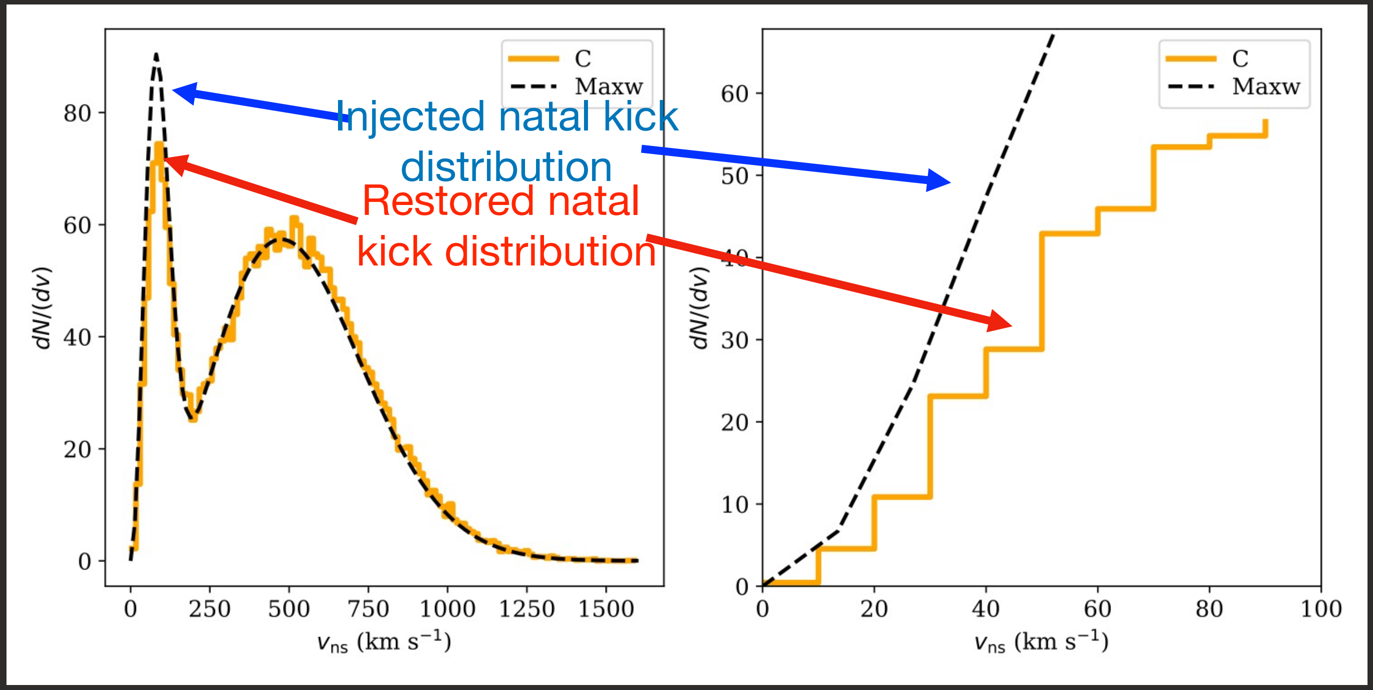

Formation path

		M_1	M_2	t (Myr)	P
	MSMS	11.85	8.27	0.0	40.1 yrs
	HGMS	11.67	8.26	18.0	40.9 yrs
THRM	HGMS	11.67	8.26	18.0	67.3 ds
	HdMS	2.69	8.33	18.0	34.8 ds
	HgMS	2.49	8.33	21.0	36.1 ds
	NSMS	1.38	8.33	21.0	0.3 yrs
	NSHG	1.38	8.24	35.0	0.3 yrs
	NSHG	1.38	8.24	35.0	55.7 ds
	NSHd	1.38	1.68	35.0	7.0 hrs
	NSHg	1.38	1.62	42.0	7.3 hrs
THRM	NSHg	1.38	1.6	42.0	7.4 hrs
	NSWD	1.38	0.9	42.0	0.6 ds

Be X

Isolated radio pulsar

Other formation paths

		M_1	M_2	t (Myr)	P
	MSMS	14.47	0.68	0.0	6.4 yrs
	HGMS	14.11	0.68	13.0	6.7 yrs
	hbMS	14.09	0.68	13.0	6.7 yrs
	SgMS	12.16	0.68	15.0	5.3 yrs
CE	SgMS	12.16	0.68	15.0	5.3 yrs
	HgMS	4.56	4.48	15.0	4.0 ds
	NSMS	1.55	4.48	15.0	13.5 ds
	NSHG	1.55	4.48	151.0	9.0 ds
THRM	NSHG	1.55	4.48	151.0	9.0 ds

Dynamically unstable mass transfer (CE) - probably not enough angular momentum is transferred to B star, so decression disk is never formed, NS has nothing to accrete.

	M_1	M_2	t (Myr)	P
MSMS	14.53	3.31	0.0	635.3 yrs
HGMS	14.17	3.31	13.0	661.4 yrs
hbMS	14.15	3.31	13.0	662.9 yrs
SgMS	12.2	3.31	15.0	840.2 yrs
NSMS	1.52	3.31	15.0	445.8 yrs
NSHG	1.52	3.31	291.0	445.8 yrs
NSsg	1.52	3.31	293.0	445.8 yrs
NShb	1.52	3.31	294.0	446.1 yrs
NSSg	1.52	3.28	358.0	451.0 yrs
NSWD	1.52	0.78	362.0	1137.9 yrs
NSWD	1.52	0.78	100000.0	1137.9 yrs

Isolated stellar evolution - two stars never transfer any mass. B star cannot gain angular momentum, so decression disk is never formed, NS has nothing to accrete.

Other formation paths

Mixed channel - multiple mass transfers, some stable and some dynamically unstable. The outcome is unclear. This is a rare channel.

Exploratory models

Model	Natal kick	Remnant mass	Mass accretion efficiency	ecSN	Mass range for ecSN	$2\Delta\mathcal{L}$	N_{SMC}
A	Hobbs	Fryer	Default	No		99.98	200
B	Hobbs	Antoniadis	Default	No		107.8	210
C	Igoshev	Fryer	Default	No		50.44	320
D	Igoshev	Fryer	Semiconservative	No		1.3	180
E	No kick	Fryer	Semiconservative	No		20802.4	820
F	Hobbs	Fryer	Semiconservative	No		11.9	60
G0	Hobbs	Fryer	Semiconservative	Yes	1.83-2.25 ($*$)	12.4	90
G1	Hobbs	Fryer	Semiconservative	Yes	1.83-2.25	8.82	100
H0	Hobbs	Fryer	Semiconservative	Yes	1.63-2.45 ($*$)	10.9	170
H1	Hobbs	Fryer	Semiconservative	Yes	1.63-2.45	7.84	180
J0	Hobbs	Fryer	Semiconservative	Yes	1.6-2.25 ($*$)	10.66	90
J1	Hobbs	Fryer	Semiconservative	Yes	1.6-2.25	6.22	100
K	Optimum	Fryer	Semiconservative	No		-	140
L	New ecSN	Fryer	Semiconservative	Yes	1.63-2.45	5.18	140

Binary properties of each channel

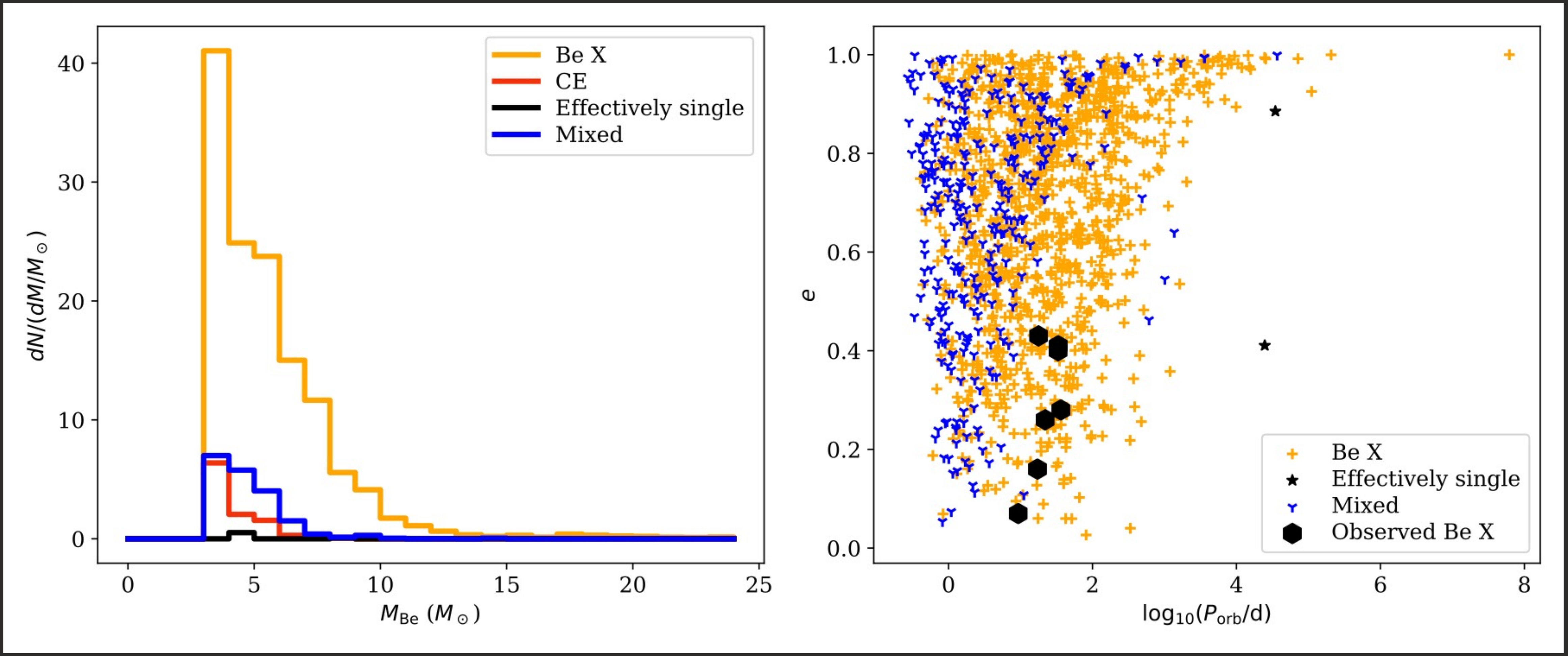

Model A: Hobbs (2006) natal kick, non-conservative mass transfer, SMC metallicity and star formation history. Black hexagonsare locations of observed Be X-ray binaries in SMC by Coe & Kirk (2015)

Binary properties of each channel

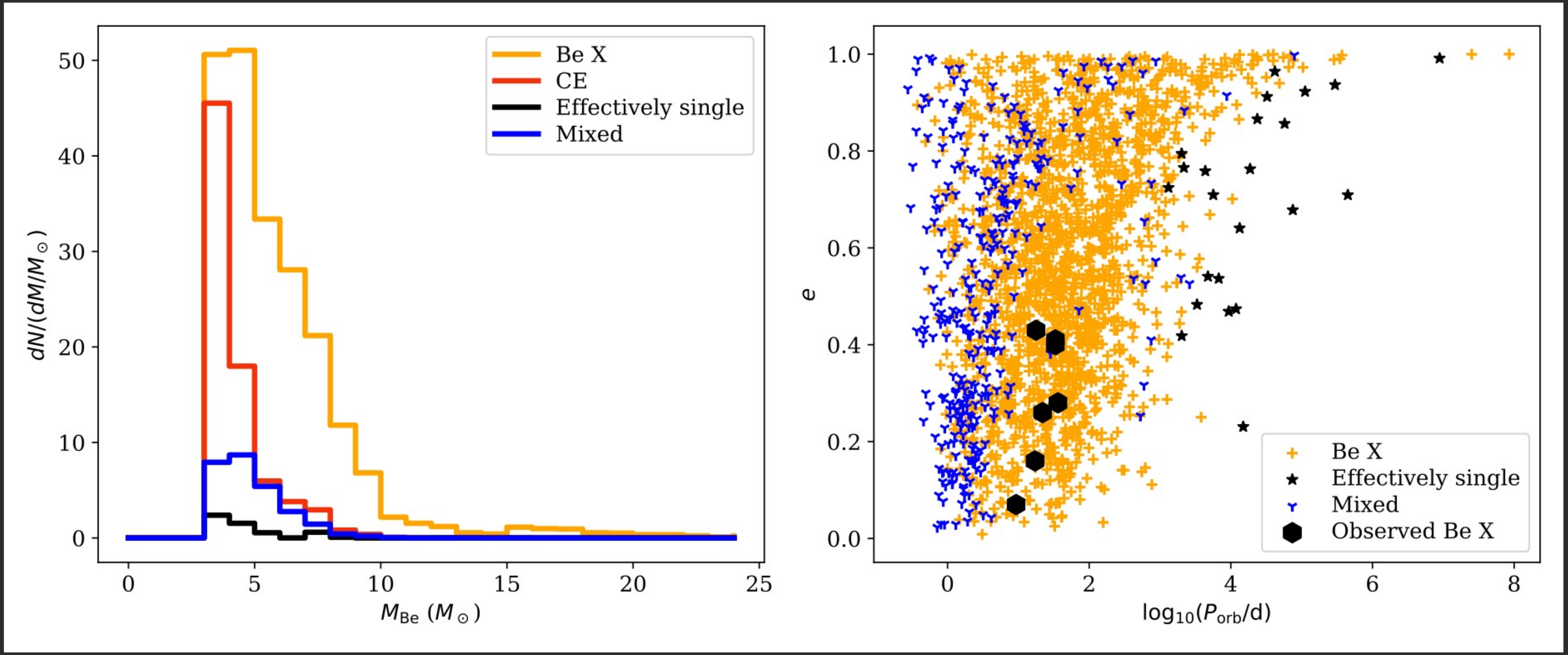

Model C: Igoshev (2020) natal kick, non-conservative mass transfer, SMC metallicity and star formation history

Binary properties of each channel

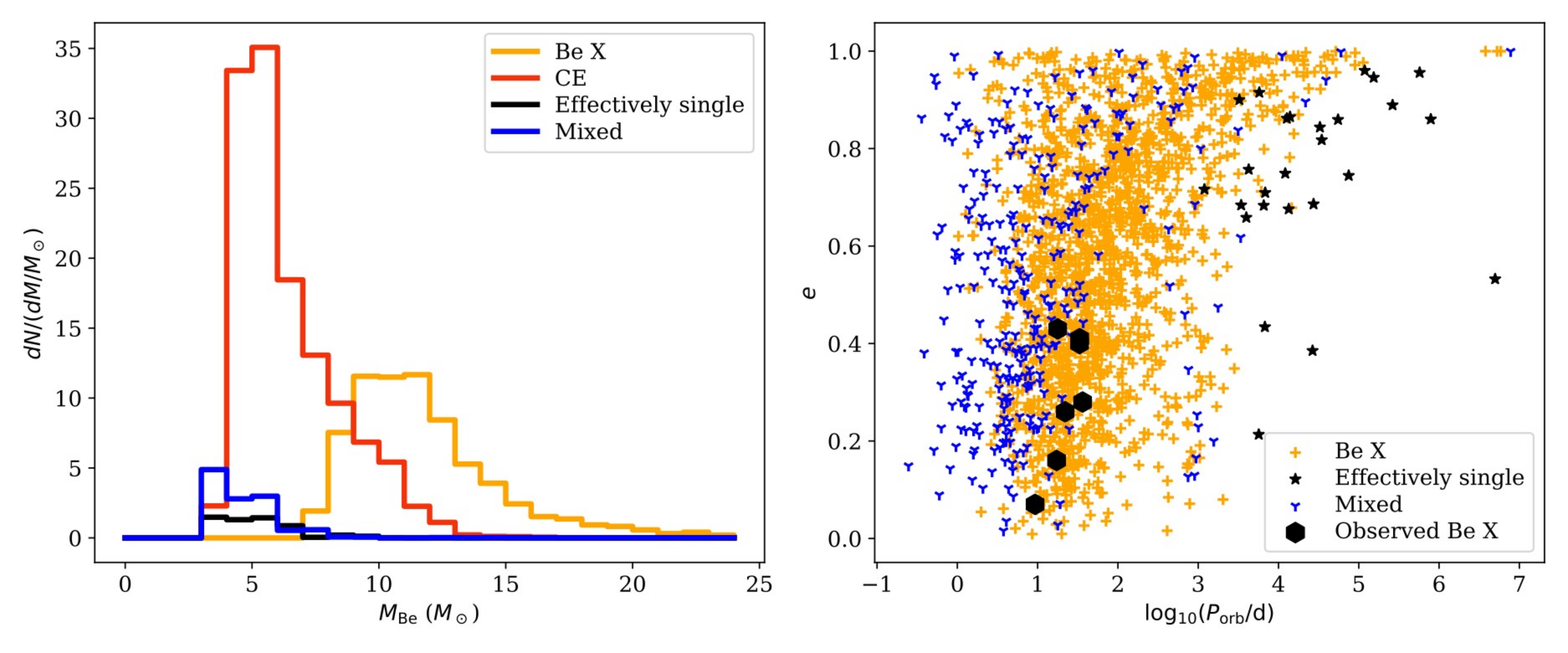

Model D: Igoshev (2020) natal kick, semi-conservative mass transfer, SMC metallicity and star formation history

Binary properties of each channel

Correlation between e and

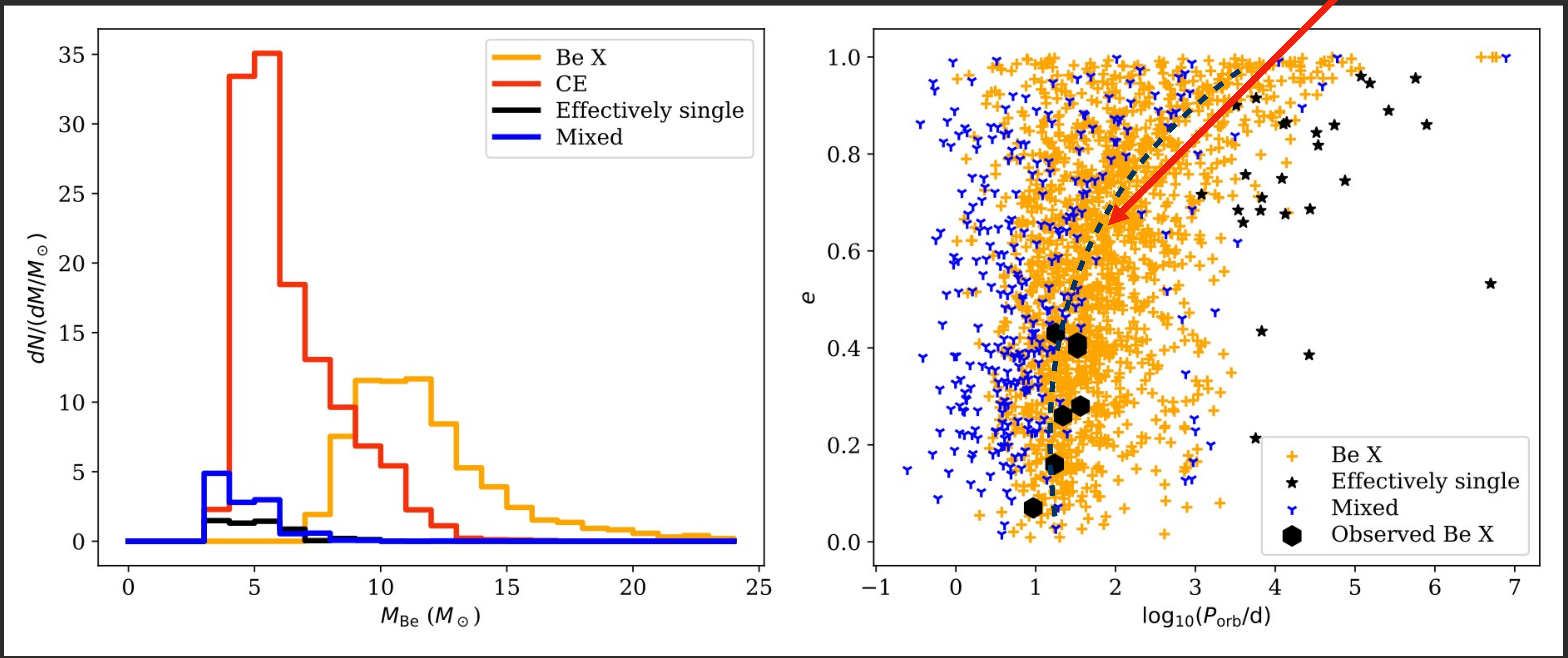

Model D: Igoshev (2020) natal kick, semi-conservative mass transfer, SMC metallicity and star formation history

Binary properties of each channel

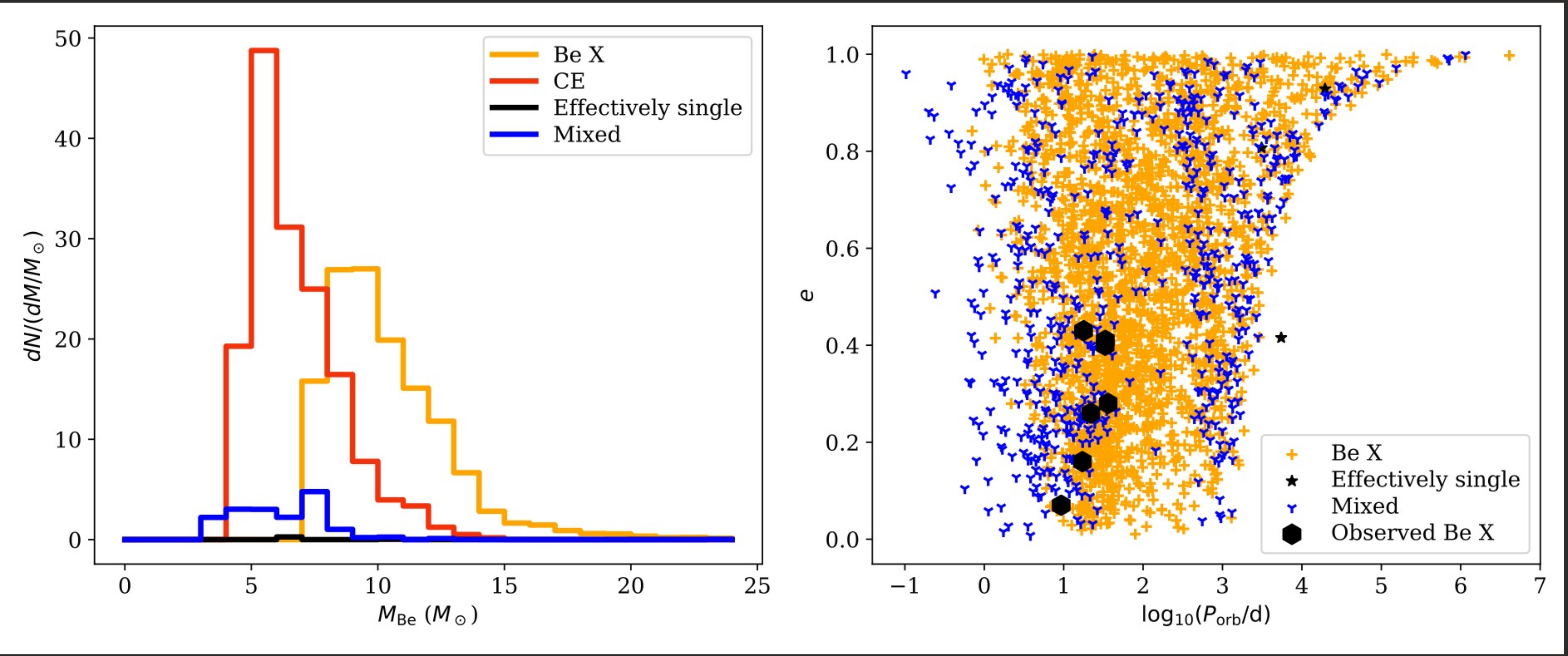

Model H: Hobbs (2006) natal kick, semi-conservative mass transfer, SMC metallicity and star formation history, ecSN

Be X-ray binaries of Milky Way and Gaia EDR3

HMXB	Sp. type	Gaia counterpart Gaia EDR3 ID	V (mag)	g (mag)	$\varpi \pm \sigma_\varpi$ (mas)	$\mu_\alpha \pm \sigma_\alpha$ (mas / year)	$\mu_\delta \pm \sigma_\delta$ (mas/year)
HD 100199	B0/1(III)n(e)	5333660129603575808	8.17	8.13	0.573 ± 0.047	−6.098 ± 0.048	1.373 ± 0.048
KRL2007b 335	O9Ia	4258160560148155648	14.06	12.76	0.164 ± 0.024	−1.366 ± 0.024	−5.595 ± 0.022
GRO J2058+42	O9.5-B0IV-Ve	2065653598916388352	14.74	14.13	0.078 ± 0.015	−2.21 ± 0.015	−3.351 ± 0.017
LS 1698	B0III/V:e	5352018121173519488	11.48	11.24	0.171 ± 0.016	−6.305 ± 0.021	3.01 ± 0.018
UCAC2 39636510	B0.5Ve	3423526544838563328	12.21	12.17	0.138 ± 0.018	0.573 ± 0.02	−0.608 ± 0.014
LS I +61 303	B0Ve	465645515129855872	10.75	10.4	0.378 ± 0.013	−0.423 ± 0.011	−0.256 ± 0.012
UCAC2 4813819	B2III/B0V	5335021599905643264	13.4	14.73	0.242 ± 0.021	−3.448 ± 0.021	1.165 ± 0.021
Ginga 0834-430	B0-2III-Ve	5523448274762133632	20.4	19.17	1.105 ± 0.217	−3.235 ± 0.215	3.755 ± 0.266
KRL2007b 84	B0e	5258414192353423360	15.27	13.88	0.243 ± 0.013	−4.702 ± 0.016	3.559 ± 0.014
2E 1752	O9.7Ve	3052677318793446016	10.9	11.99	0.154 ± 0.015	−0.638 ± 0.015	1.256 ± 0.014
GSC 03588-00834	B0Ve	2162805896614571904	14.2	13.77	0.131 ± 0.013	−3.505 ± 0.014	−3.16 ± 0.013
V* V635 Cas	B0.2Ve	524677469790488960	15.19	14.3	0.136 ± 0.016	−1.684 ± 0.013	0.504 ± 0.017
V* BQ Cam	O8.5Ve	444752973131169664	15.42	14.2	0.134 ± 0.02	−0.268 ± 0.02	0.44 ± 0.02
HD 34921	B0IVpe	184497471323752064	7.48	7.23	0.721 ± 0.03	1.305 ± 0.041	−3.999 ± 0.028
2MASS J17002524-4219003	B2e	5966213219190201856	9.15	8.71	0.641 ± 0.023	1.181 ± 0.03	−1.47 ± 0.023
V* V441 Pup	O5Ve	5613494119551805184	11.83	11.6	0.096 ± 0.017	−0.881 ± 0.012	1.785 ± 0.018
AX J1739.1-3020	O8.5Iab(f)	4056922100878037120	14.8	16.22	0.68 ± 0.053	2.954 ± 0.062	1.821 ± 0.041
BD+53 2790	O9.5Vep	2005653524280214400	9.84	9.74	0.305 ± 0.014	−4.173 ± 0.015	−3.317 ± 0.014
V* V572 Pup	B0.2IVe	5548261400354128768	12.74	12.42	0.118 ± 0.012	−1.455 ± 0.011	2.146 ± 0.016
HD 249179	B5ne	3431561565357225088	10.0	10.01	0.597 ± 0.03	0.634 ± 0.034	−2.189 ± 0.021
V* GP Vel	B0.5Ia	5620657678322625920	6.87	6.74	0.496 ± 0.015	−4.822 ± 0.015	9.282 ± 0.016
LS V +44 17	B0.2Ve	252878401557369088	10.73	10.4	0.379 ± 0.015	0.101 ± 0.016	−1.186 ± 0.014
SS 188	OB	5541793213959987968	12.33	12.16	0.178 ± 0.01	−2.367 ± 0.009	3.177 ± 0.013
V* V479 Sct	ON6V((f))z	4104196427943626624	11.27	10.8	0.49 ± 0.015	7.425 ± 0.014	−8.151 ± 0.012
BD+60 73	B1Ib	427234969757165952	9.66	9.45	0.272 ± 0.012	−1.796 ± 0.011	−0.525 ± 0.014
EM* AS 14	B2	414196617287885312	11.36	11.41	0.339 ± 0.018	−2.463 ± 0.015	−0.546 ± 0.017
4U 2238+60	Be	2201091578667140352	14.8	14.1	0.104 ± 0.014	−2.344 ± 0.015	−1.015 ± 0.014
EM* GGA 104	B1IIIe	511220031584305536	11.42	11.22	0.328 ± 0.022	−1.029 ± 0.016	−0.082 ± 0.017
V* V662 Cas	B1Iae	524924310153249920	11.14	10.52	0.196 ± 0.011	−1.243 ± 0.009	0.761 ± 0.012
2MASS J01581848+6713234	B2IVe+	518990967445248256	14.43	13.69	0.133 ± 0.013	−1.198 ± 0.011	0.3 ± 0.013
HD 74194	O8.5Ib-II(f)p	5522306019626566528	7.55	7.45	0.443 ± 0.017	−7.465 ± 0.02	6.1 ± 0.019
HD 63666	B7IV/V	5489434710755238400	7.6	7.54	1.536 ± 0.021	−4.572 ± 0.027	8.53 ± 0.028
WRAY 15-793	O9.5III/Ve	5336957010898124160	12.12	11.59	0.329 ± 0.011	−5.421 ± 0.012	1.37 ± 0.012
V* QV Nor	B0.2Ia:e	5886085557746480000	14.5	13.16	0.128 ± 0.015	−6.711 ± 0.015	−4.111 ± 0.014
HD 49798	sdO6	5562023884304074240	8.287	8.22	1.92 ± 0.05	−4.162 ± 0.066	5.926 ± 0.058
V* CI Cam	B0/2I[e]	276644757710014976	11.77	10.77	0.21 ± 0.015	−0.474 ± 0.018	−0.51 ± 0.013
V* BP Cru	B1.5Iaeq	6054569565614460800	10.66	9.75	0.251 ± 0.016	−5.227 ± 0.016	−2.071 ± 0.019
HD 245770	O9/B0III/Ve	3441207615229815040	9.39	8.6	0.525 ± 0.023	−0.59 ± 0.031	−2.88 ± 0.016
IGR J17544-2619	O9Ib	4063908810076415872	12.94	11.66	0.396 ± 0.027	−0.506 ± 0.029	−0.668 ± 0.018
SS 433	A7Ib:	4293406612283985024	13.0	12.6	0.118 ± 0.023	−3.027 ± 0.024	−4.777 ± 0.024
HD 226868	O9.7Iabpvar	2059383668236814720	8.91	8.54	0.444 ± 0.015	−3.812 ± 0.015	−6.31 ± 0.017
CPD-63 2495	O9.5Ve	5862299960127967488	9.98	9.63	0.443 ± 0.013	−7.093 ± 0.012	−0.342 ± 0.014

Identified more than 40 HMXBs in data of Gaia EDR3 with precise enough measurements of parallax and proper motion. All of these are located in the Milky Way.

Comparison of simulated peculiar velocities with observations

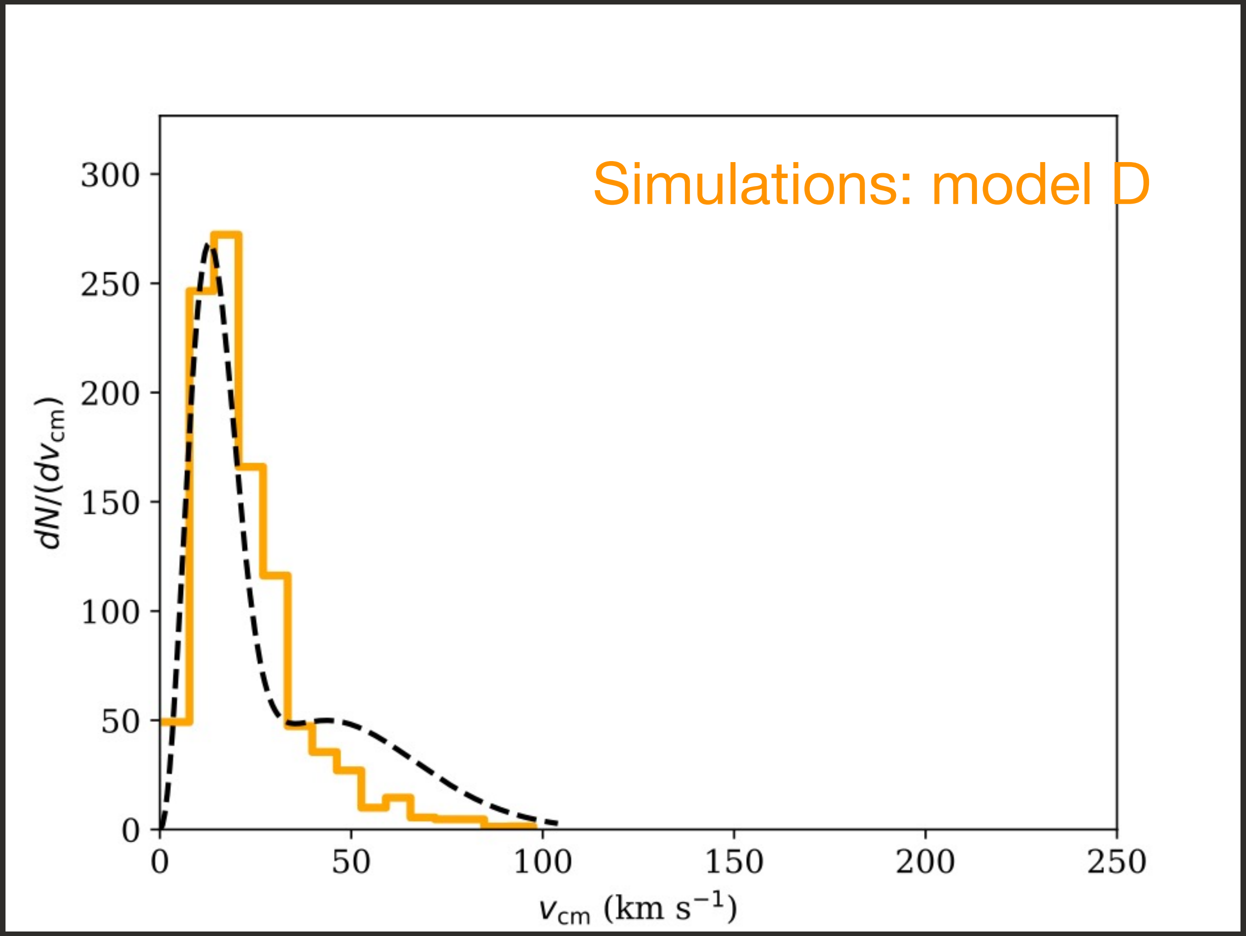

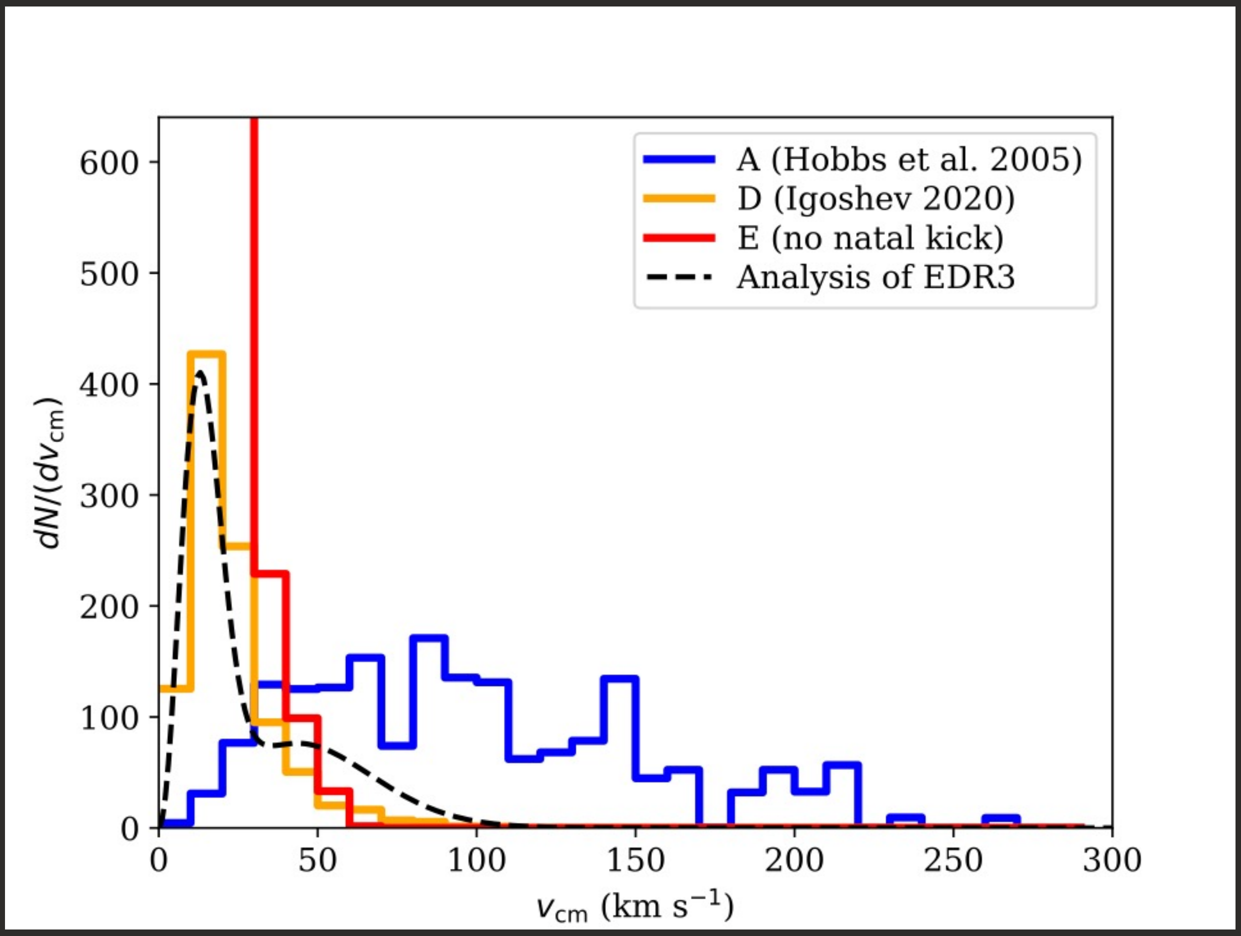

Model D

- Model D fits well all available observational constrains:
- (1) a peak of Be masses is located around 11~M$_\odot$,
- (2) it produces ~130 Be X-ray binaries in SMC (compatible with estimates of 120 HMXBs),
- (3) Be X-ray binaries with measured periods and eccentricities coincide with maximum density of simulated systems
- (4) it produces natal kick for isolated radio pulsars mostly compatible with Igoshev (2020)
- (5) systemic velocities of Galactic Be X-ray binaries follow quite closely the simulations

Combined analysis

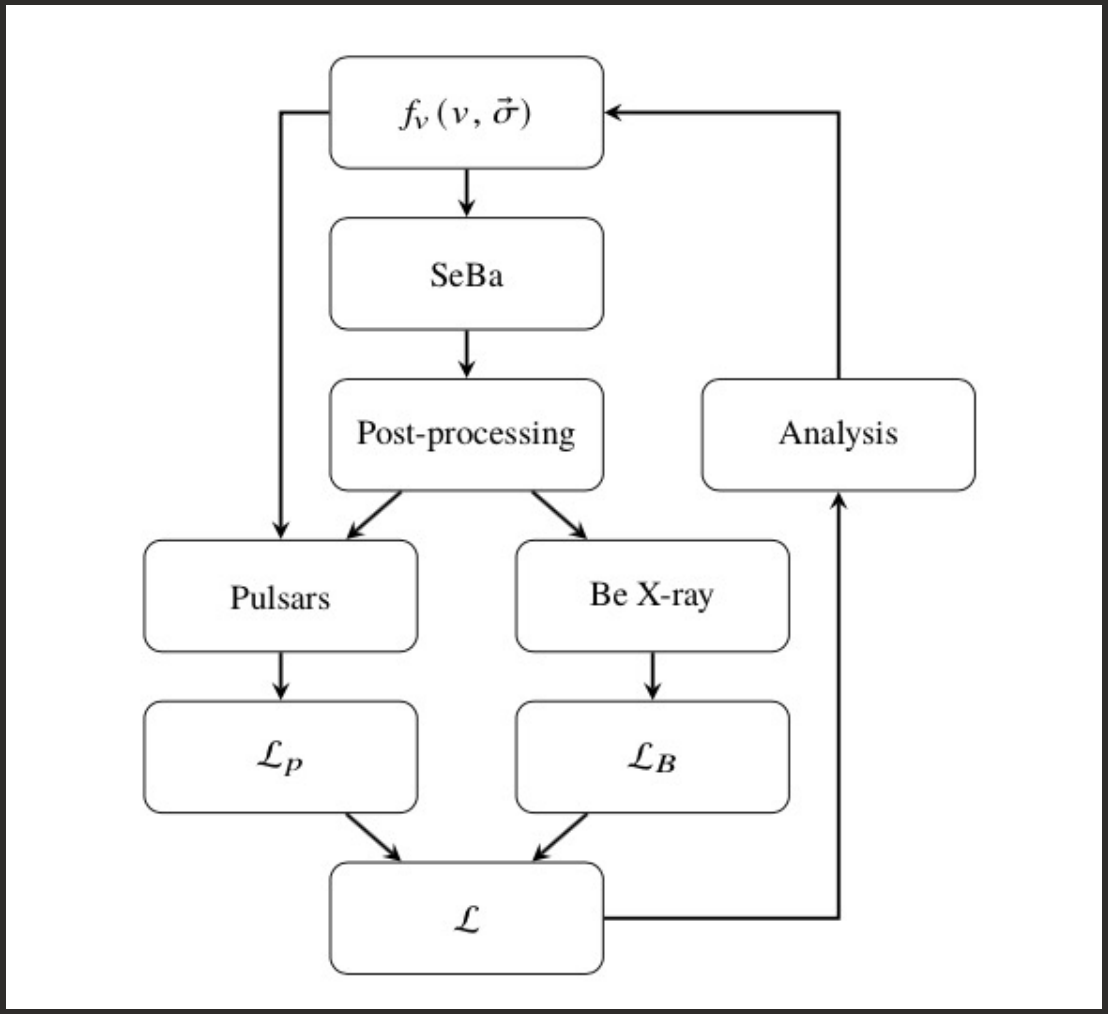

Simulations: binned likelihood

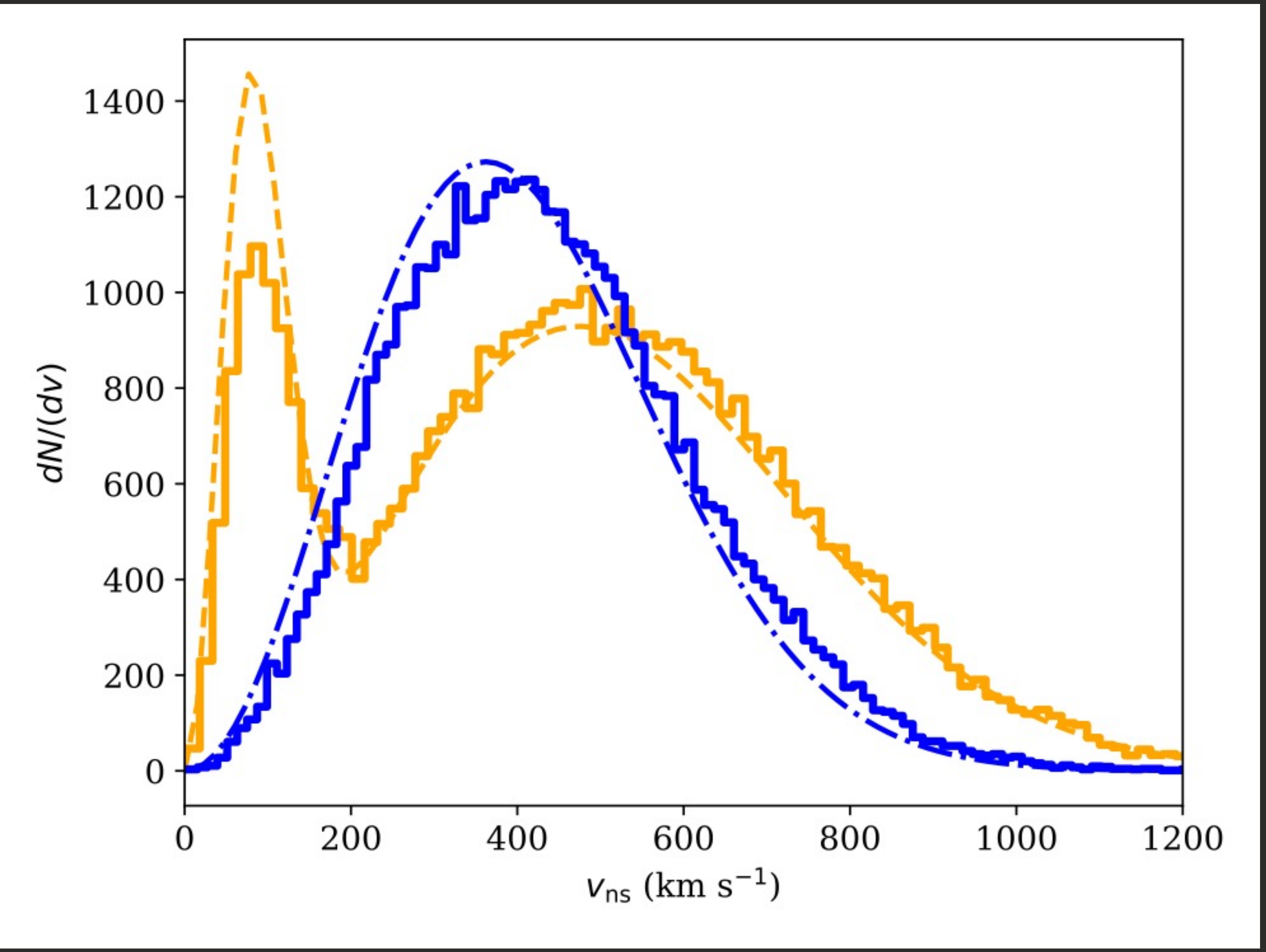

$$f_v(\vec{m}) = \sum_{i=1}^{N} m_i v^2 v_h(v)$$

$$\int_0^\infty f_v(\vec{m})dv = \sum_{i=1}^{N} m_i \Delta v^3 \left(\frac{(i+1)^3 - i^3}{3}\right) = 1$$

$$P_{\rm maxw}(\varpi', \mu'_{\alpha*}, \mu'_\delta, D, v_\alpha, v_\delta, v_r) = G(v_\alpha, \sigma)G(v_\delta, \sigma)G(v_r, \sigma)$$
$$\times \frac{f_D(D)}{\int_0^{D_{\rm max}} f_D(D)dD} \frac{1}{\sigma_\varpi\sqrt{2\pi}} \exp\left[-\frac{(1/D - \varpi')^2}{2{\sigma_\varpi}^2}\right]$$
$$\times \frac{1}{\sigma_\alpha\sqrt{2\pi}} \exp\left[-\frac{(\mu_{\alpha*,G}(D) + v_\alpha/D - \mu'_{\alpha*})^2}{2{\sigma_\alpha}^2}\right]$$
$$\times \frac{1}{\sigma_\delta\sqrt{2\pi}} \exp\left[-\frac{(\mu_{\delta,G}(D) + v_\delta/D - \mu'_\delta)^2}{2{\sigma_\delta}^2}\right]$$

Combined analysis

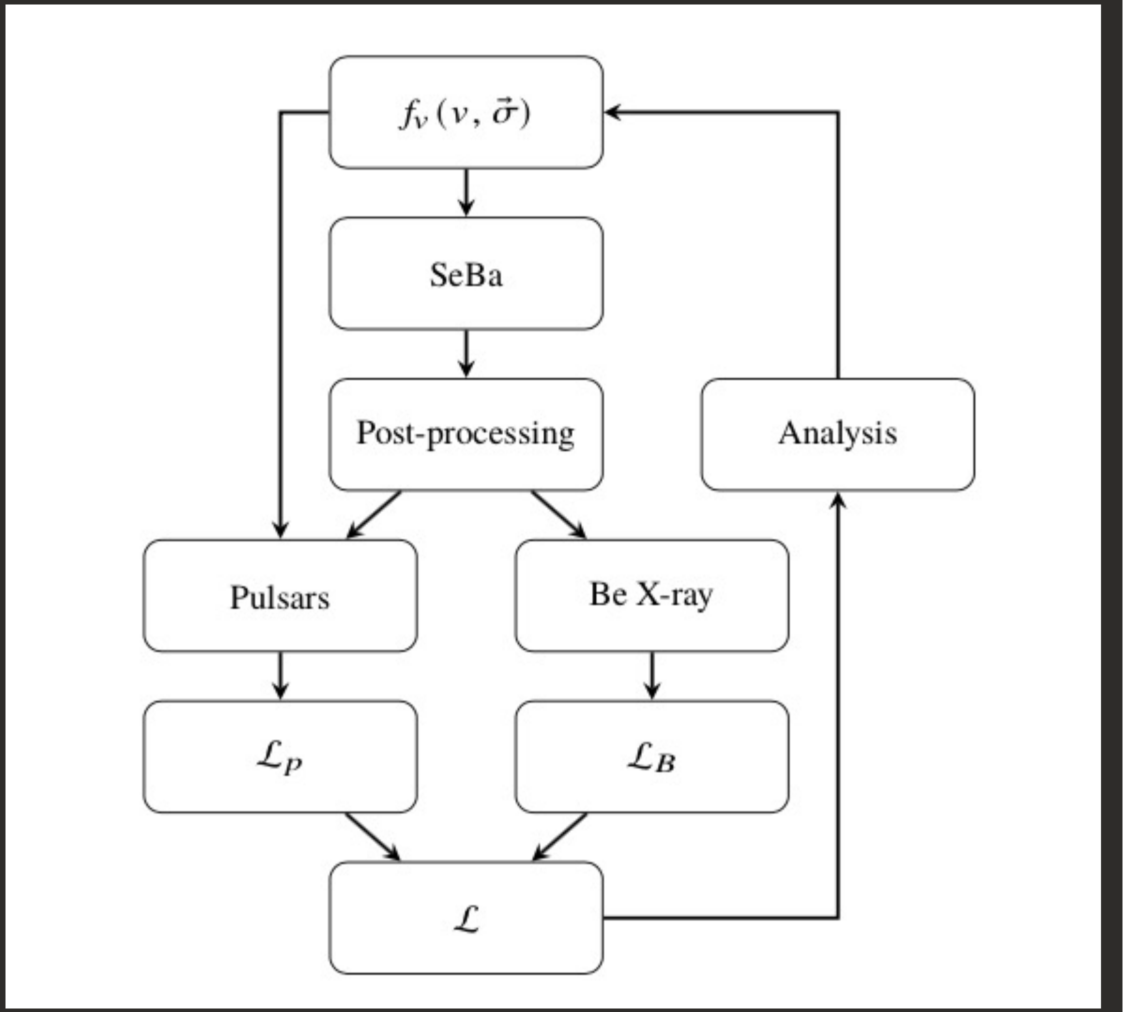

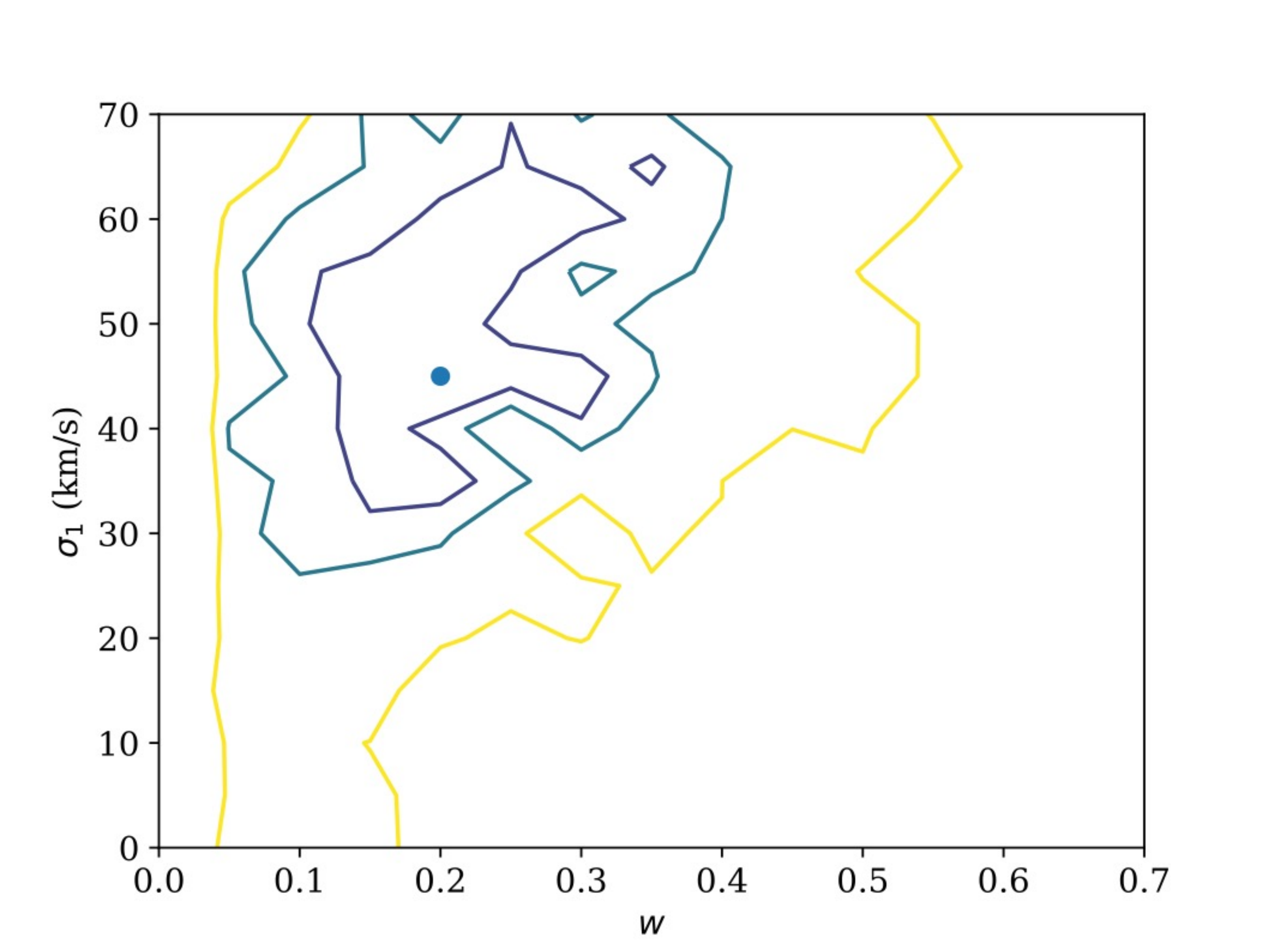

Combined analysis

Isolated pulsar likelihood profiles

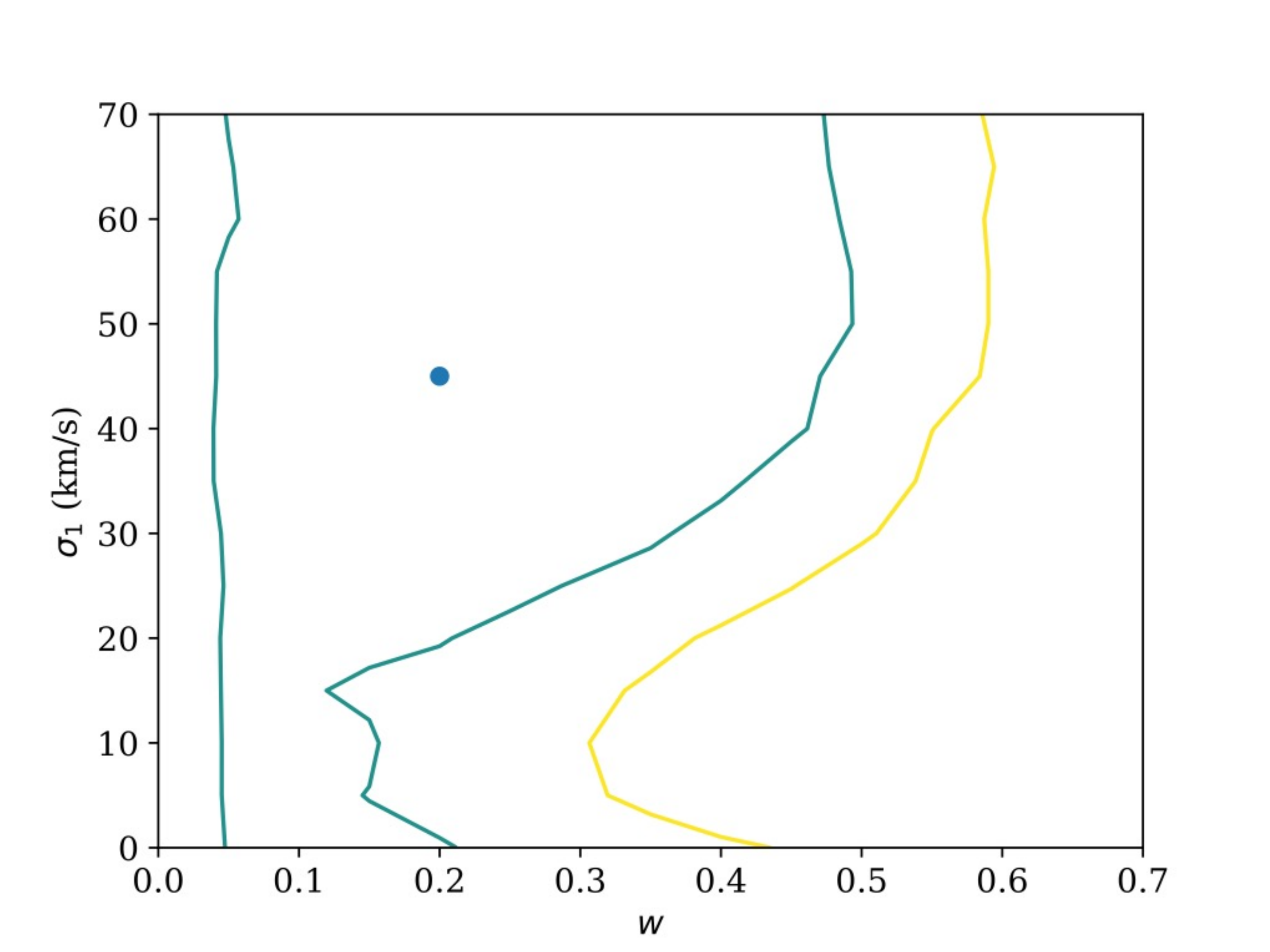

Be X-ray likelihood profiles

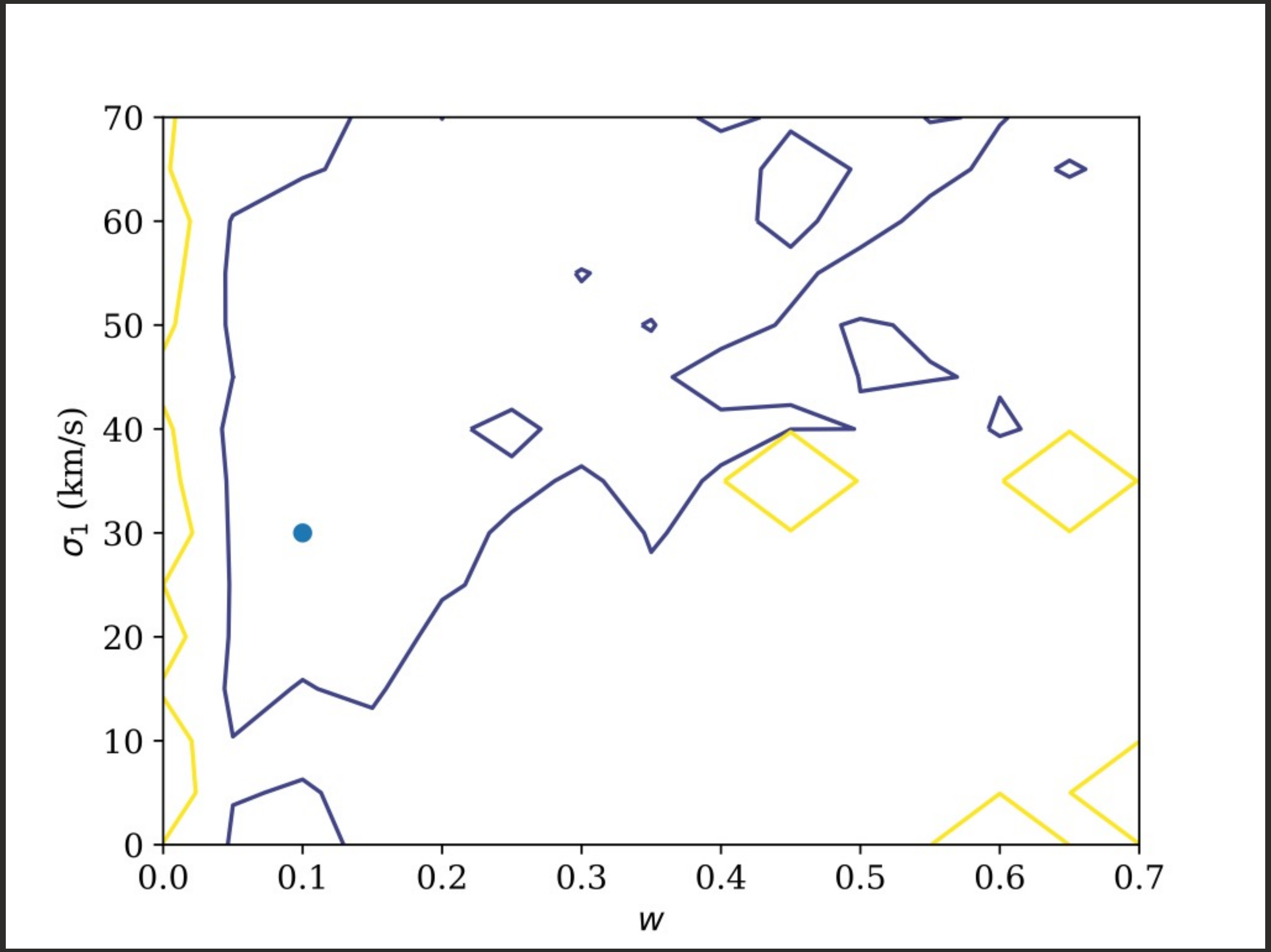

Combined analysis

Isolated pulsar likelihood profiles

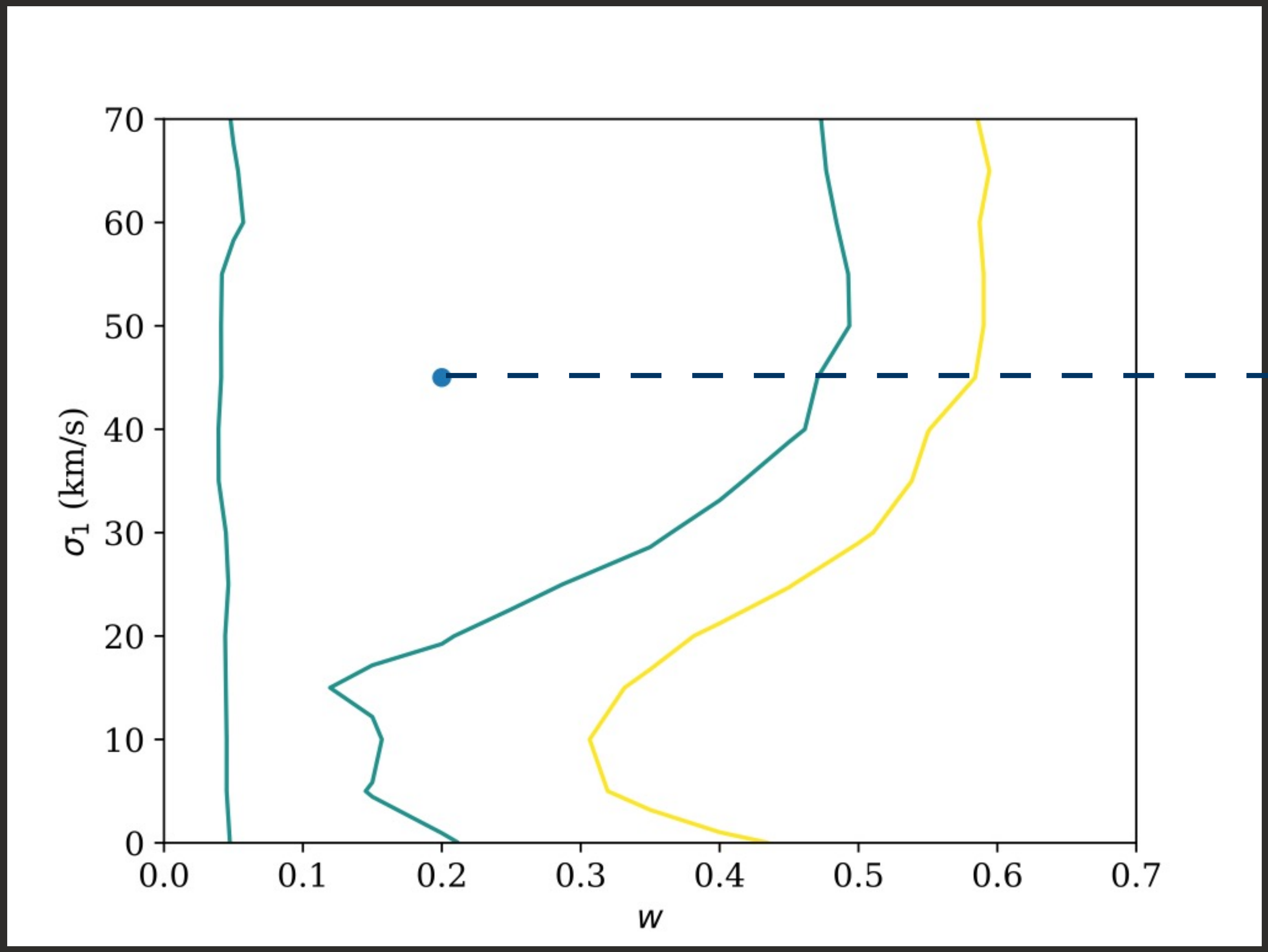

Be X-ray likelihood profiles

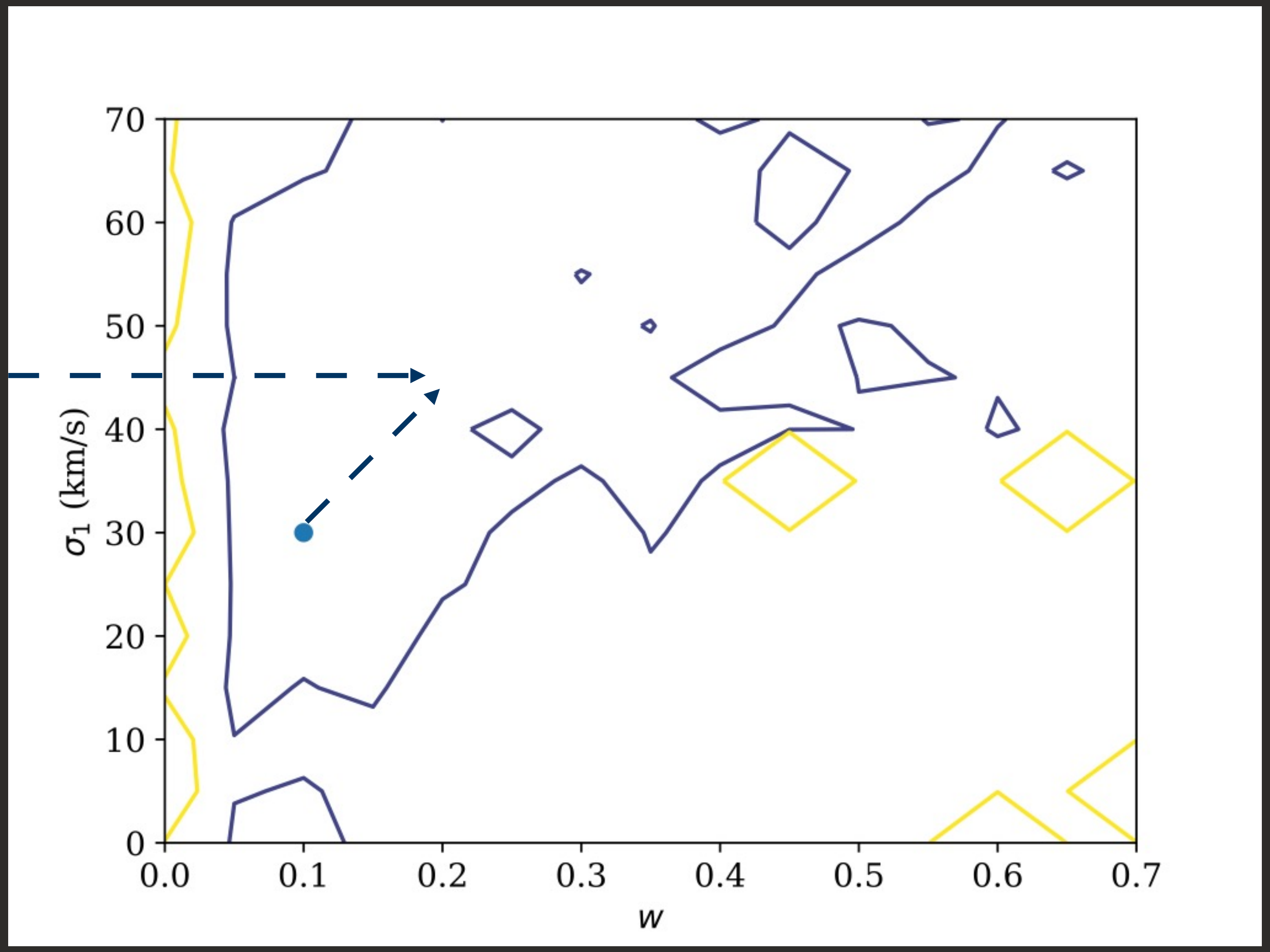

Combined analysis

Isolated pulsar likelihood profiles

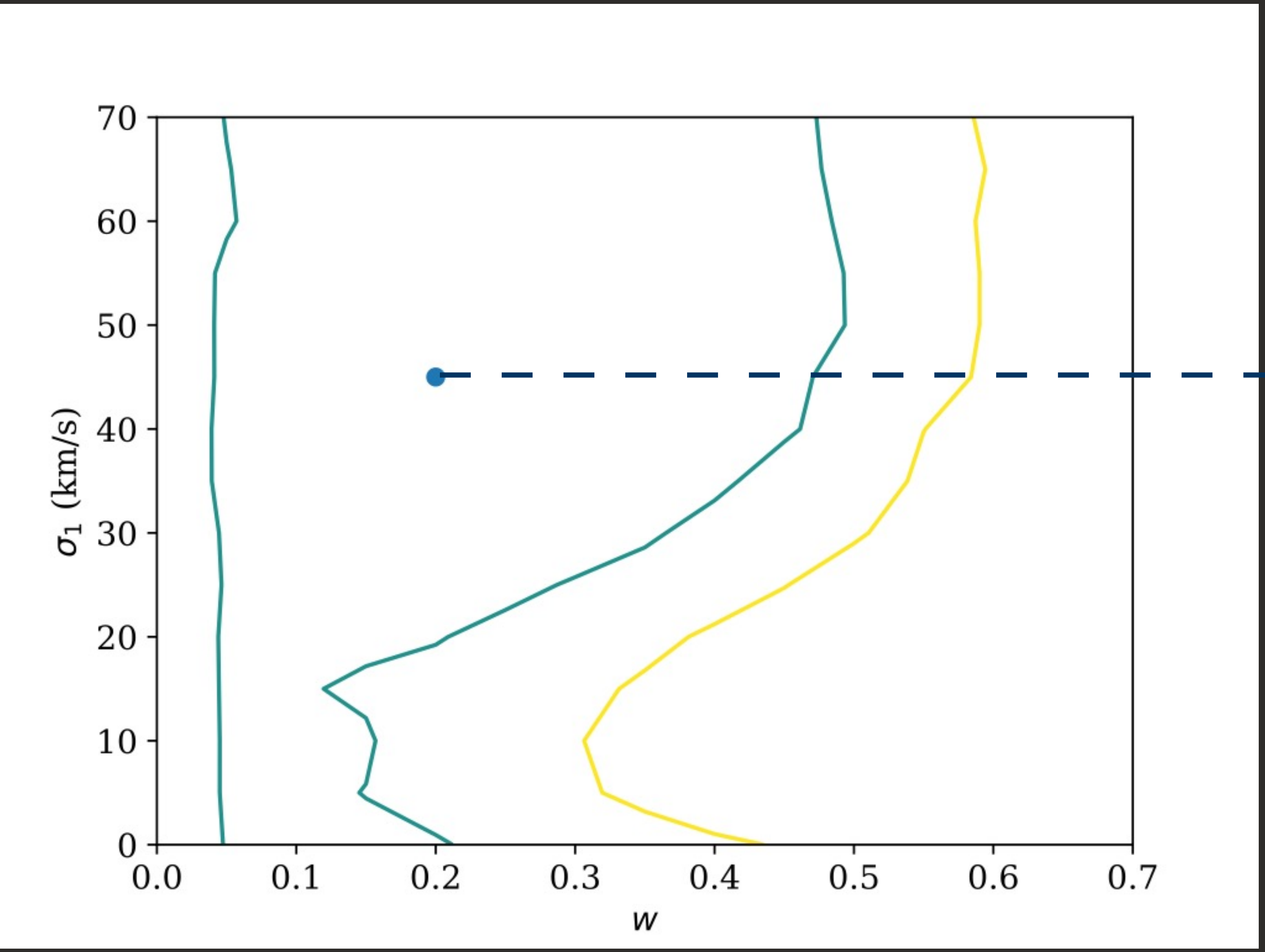

Be X-ray likelihood profiles

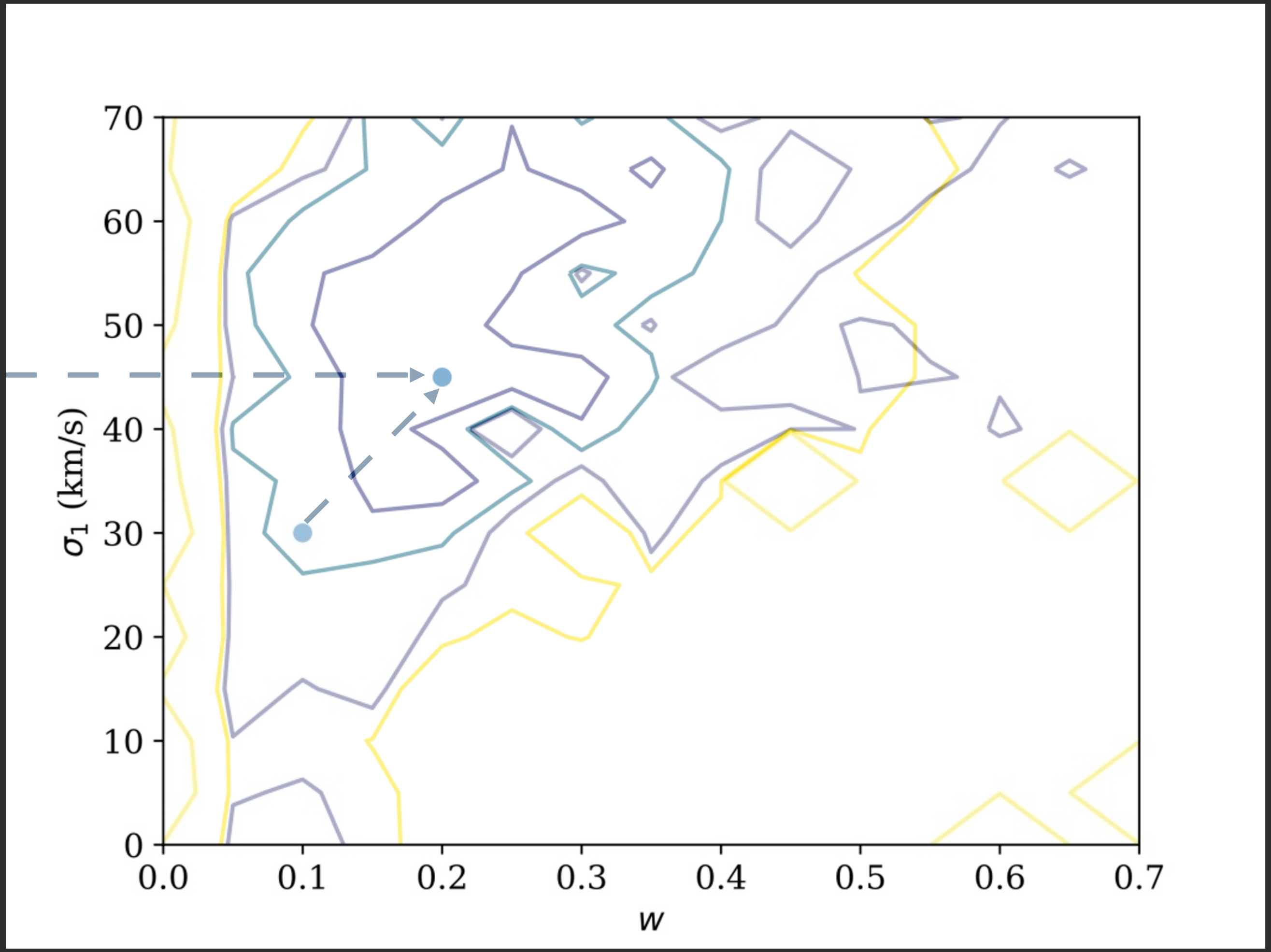

Electron capture supernova explosions

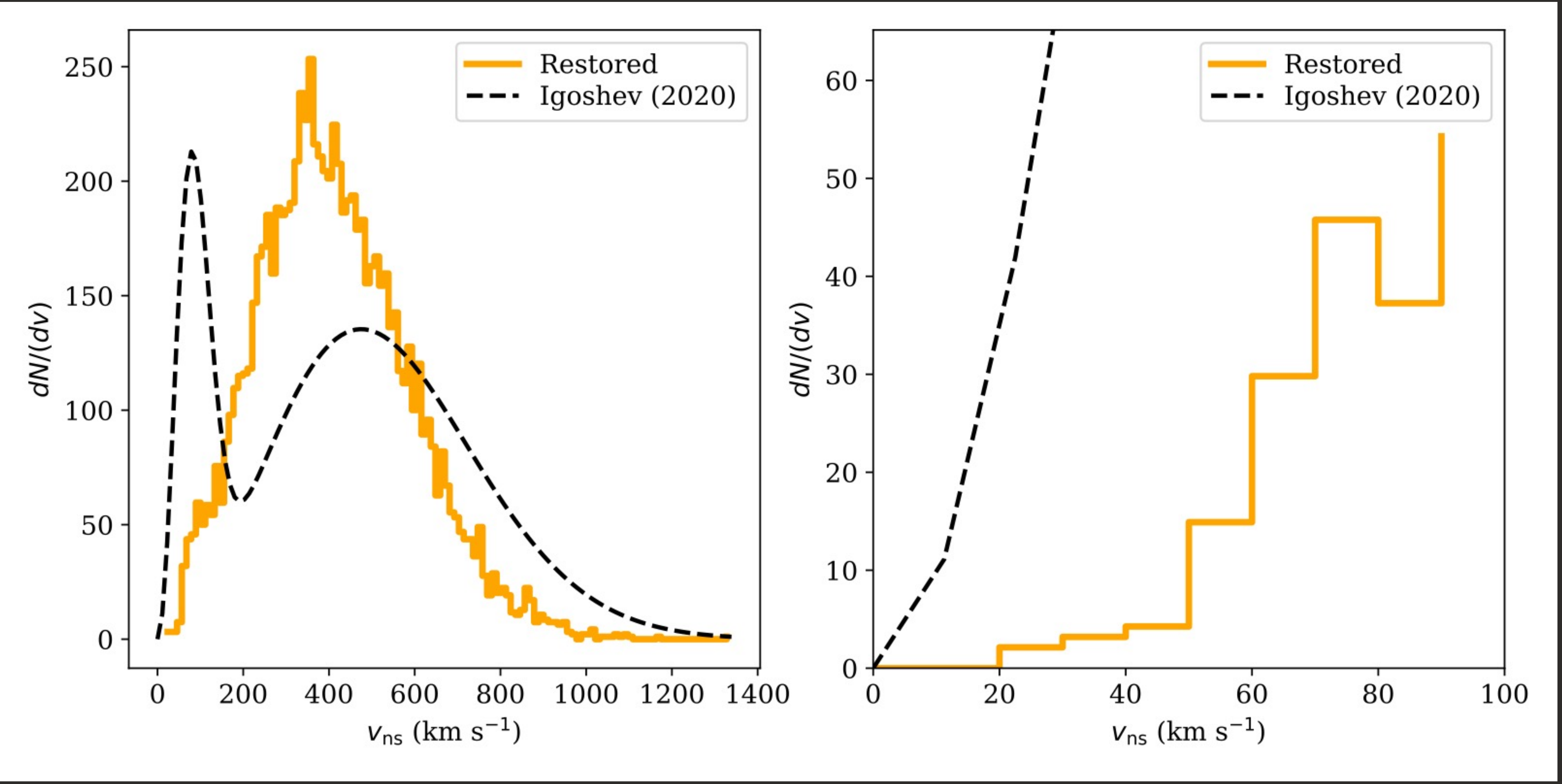

Electron capture supernova explosions

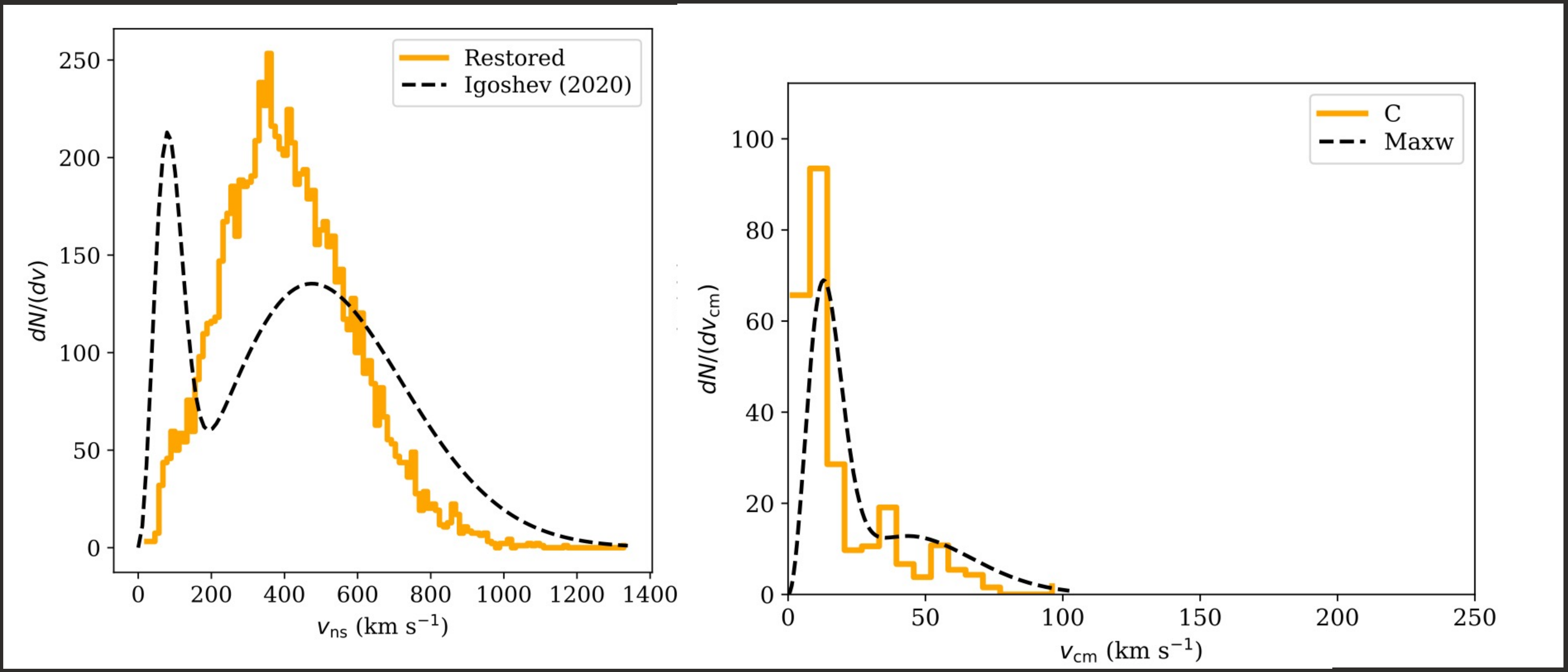

Electron capture supernova explosions

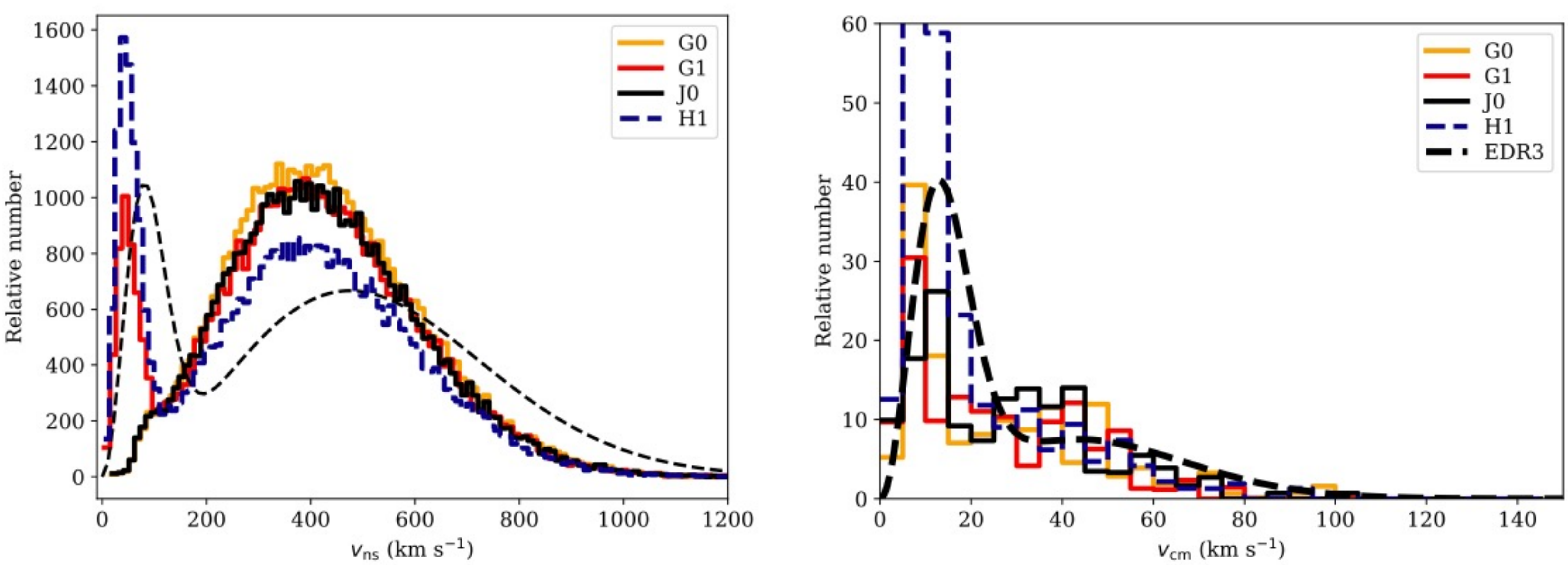

Conclusions

- Model D successfully satisfies multiple observational constraints based on observations of Galactic isolated radio pulsars and Be X-ray binaries as well as Be X-ray binaries in SMC.
- It is possible to slightly improve this result by using w=0.2 and $\sigma_1 = 45$ km/s
- ecSN does not give correct predictions for velocity distribution of isolated radio pulsars

Thank you for your attention!